

CT
EPT
100

DOT/FAA/CT-82/100

FAA WJH Technical Center
00090267

NBSIR 82-2508

An Assessment of Correlations Between Laboratory and Full-Scale Experiments for the FAA Aircraft Fire Safety Program, Part 1: Smoke

FEDERAL AVIATION ADMINISTRATION

AUG 18 1983

TECHNICAL CENTER LIBRARY
ATLANTIC CITY, N.J. 08405

U.S. DEPARTMENT OF COMMERCE
National Bureau of Standards
National Engineering Laboratory
Center for Fire Research
Washington, DC 20234

July 1982

Sponsored by:
**U.S. Department of Transportation
Federal Aviation Administration
Technical Center
Atlantic City Airport, NJ 08405**

NBSIR 82-2508

**AN ASSESSMENT OF CORRELATIONS
BETWEEN LABORATORY AND
FULL-SCALE EXPERIMENTS FOR THE
FAA AIRCRAFT FIRE SAFETY PROGRAM,
PART 1: SMOKE**

James G. Quintiere

U.S. DEPARTMENT OF COMMERCE
National Bureau of Standards
National Engineering Laboratory
Center for Fire Research
Washington, DC 20234

July 1982

Sponsored by:



U.S. Department of Transportation
Federal Aviation Administration
Technical Center
Atlantic City Airport, NJ 08405



U.S. DEPARTMENT OF COMMERCE, Malcolm Baldrige, *Secretary*
NATIONAL BUREAU OF STANDARDS, Ernest Ambler, *Director*

AN ASSESSMENT OF CORRELATIONS BETWEEN LABORATORY
AND FULL-SCALE EXPERIMENTS FOR THE FAA AIRCRAFT
FIRE SAFETY PROGRAM, PART 1: SMOKE

by

James G. Quintiere

Abstract

An extensive review is presented demonstrating the nature of comparison between full-scale fire smoke data and test method results for materials. These correlations are presented in terms of consistent parameters established through a development of the governing equations for smoke concentration and light attenuation. Visibility data limited to light transmission through smoke are also presented. The complex dependence of smoke production on many parameters acting in fire growth limits the success of simple correlation methods. Recommendations are made for further research to establish a sound basis for correlations, and the prediction of smoke obscuration due to fire.

Key words: Correlation, full-scale, review, smoke, test methods

TABLE OF CONTENTS

	Page
INTRODUCTION	1
Purpose	1
Background	1
DISCUSSION	2
Visibility in Smoke	2
Macroscopic Equations for Smoke and Optical Density	3
Factors Affecting Smoke Properties	8
COMPARISON BETWEEN TEST (METHOD) DATA AND LARGE SCALE FIRE EXPERIMENTS	11
Comparisons for Closed Systems	12
Comparisons with Fullscale Room Fire Growth Data	12
Comparison Between Test Methods	15
CONCLUSIONS	16
REFERENCES	19
APPENDIX	

LIST OF TABLES

Table		Page
A-1	Data from Heselden	A-3
A-2	Data from Watts	A-4
A-3	Data from Parker	A-5
A-4	Data from Babrauskas	A-6
A-5	Data from Woolley, Raftery, Ames, Murrell	A-7
A-6	Data from Evans	A-8
A-7	Data from Tustin	A-9

LIST OF ILLUSTRATIONS

Figure		Page
1	Visibility Results Derived from Rasbash [29], Jin [5], and Lopez [1].	22
2	Conservation of Mass for Smoke in a Control Volume (region Enclosed by dashed lines).	23
3	Mass Optical Density as a Function of Heat Flux Derived from Brown [23].	24
4	$D_{s,max}$ Rankings at two Flux Levels from Brown [23] for Piloted Ignition.	25
5	$D_{s,max}$ Compared for the Smoke Density Chamber and Large Closed Rooms from Lopez [1], Shores [32] and Robertson [33].	26
6	Comparison Between Full-Scale and Test Method Results in Terms of Maximum Specific Optical Density ($D_{s,max}$) and Mass Optical Density ($\alpha\chi$).	27
7	Smoke Production for Plywood as a Function of Temperature (a) and Ventilation Factor (b) from Saito [24].	28
8	Full-Scale Smoke Compared to D_s from the OSU Combustibility Apparatus at Several Heat Flux ^s Levels [21].	29
9	Results from Room Lining Fires Compared to the Smoke Density Chamber from Christian and Waterman [42].	30
10	Smoke in Corridor Fire Spread Compared to Results Derived from the Steiner Tunnel Test from Christian and Waterman [42].	31
11	Lining Fires in Rooms and Smoke Data from the Smoke Density Chamber and the ASTM E-84 Tunnel Classification for Smoke from Fang [43].	32
12	Smoke from Lining Fires in a Room Compared to the Early Fire Hazard (Australia) Test Method [44].	33
13	Comparison of Smoke Density Chamber, OSU Combustibility Apparatus, and British Smoke Test Data [21, 33].	34
A-1	Full-Scale Test Configurations and Test Method Apparatus Used in Correlation. Symbols Denote Measurement Locations: D-Light Transmission, T-Temperature, V-Velocity, m-Mass Loss.	A-2

NOMENCLATURE

- A - fuel surface area
- A_o - area of room opening
- C_s - mass of smoke particulate per unit gas volume
- D - optical density, Eq. (3)
- D_s - specific optical density, Eqs. (15, 16)
- \dot{E} - rate of energy release
- H_o - height of room opening
- I - light intensity
- k_a, k_s, k_v - parameters
- L - path length of light beam
- L_v - visibility, Eq. (6)
- m - mass or mass loss
- \hat{n} - unit outward normal vector
- S - surface area of control volume
- t - time
- \vec{v} - velocity vector
- V - volume
- \dot{V} - volume flow rate
- X - general abscissa variable
- Y - general ordinate variable
- α - particle optical density Eq. (12)
- δ - sample thickness
- Δ - change in (initial to final)
- σ - extinction coefficient
- χ - fraction of particulate mass to fuel mass loss

SUBSCRIPTS.

- a - absorption
- f - final
- o - initial
- s - scattering, smoke particulate
- v - visibility

SUPERSCRIPTS.

- ($\dot{\quad}$) - per unit time
- (\quad)" - per unit area

ACKNOWLEDGEMENT

This study was sponsored by the Fire Safety Branch of The Federal Aviation Administration Technical Center at Atlantic City, New Jersey. The author gratefully appreciates the advice of Mr. R. Hill, the technical monitor, and also the assistance of Mr. C. Sarkos of the FAA.

INTRODUCTION

PURPOSE.

The purpose of this review is to present and to interpret experimental smoke measurements. Comparisons will be made of data from laboratory fire tests for smoke with those of full-scale fire experiments. A positive correlation of these results could be interpreted as a basis for the relevance and credibility of the laboratory test method to measure the production of smoke in fire. Alternatively, a positive correlation could be interpreted as fortuitous since conditions in an uncontrolled fire vary while laboratory test conditions are fixed. Hence some underlying factors controlling the production of smoke must be identified to fully appreciate, and perhaps understand, the degree to which such correlation comparisons are sound.

An analytical review of the fire smoke literature was made primarily seeking studies related to comparisons between full-scale fires and test methods. It may not be totally comprehensive, but the results are believed to be representative of the state-of-the-art. Where possible, results from various studies were unified using the governing equations for smoke production and light attenuation. Studies related to the factors on which smoke production and obscuration depend were also reviewed. It is intended that the results of this study demonstrate the extent to which a laboratory test for smoke can predict smoke in an actual fire, and the factors which influence the results of a prediction or correlation. This review will not include analysis of complete fire growth computer-based models to predict smoke production (e.g. [3]).

BACKGROUND.

Smoke generation is one of the characteristics of uncontrolled fires which represents a threat to life safety. In general, smoke can be considered as the mixture of gaseous and particulate products of combustion flowing from the fire. This "smoke" could affect life safety by reducing visibility due to obscuration and by causing physiological dysfunction and other toxic effects. The two effects are related when the smoke impairs vision due to sensory irritant species produced by the fire. In fact, it has been reported that a sensory irritant effect on visibility occurred at a lower smoke concentration (optical density) than that affecting visibility for protected eyes [1]. Although a methodology has been proposed for assessing the sensory irritant effect of combustion products using an animal model [2], a clear approach to this sensory smoke hazard does not exist. In contrast, the light transmission characteristics of smoke have been studied extensively, and several methods exist for determining the "smoke contribution" of a material. It is these studies of light transmission through smoke that will be reviewed. No further discussion of the irritant and toxicological effects of smoke on vision and human function in general will be presented.

DISCUSSION

VISIBILITY IN SMOKE.

The attenuation of light by smoke is examined in order to relate it to visibility and its impact on escape from a fire. Visibility is a measure of the electromagnetic radiation in the spectral range to which the human eye is sensitive and the ability to perceive images based on their emitted, reflected and transmitted light. For the most part, smoke test methods only measure the attenuation of a parallel beam of light; they do not consider the irritant effect of smoke on vision.

Bouguer's law [4] applies to the attenuated intensity of radiation $I_\lambda(L)$ received over a path length L from a source of intensity $I_\lambda(0)$.

$$I_\lambda(L) = I_\lambda(0) \exp \left[- \int_0^L \sigma_\lambda dL' \right] \quad (1)$$

where σ_λ is the monochromatic extinction coefficient. In measurements on smoke, σ_λ is usually assumed to be uniform over the path length and independent of wavelength over the narrow band for visible radiation (or taken at a fixed wavelength if a laser light source is used). Hence

$$\sigma L = \ln \left[\frac{I(0)}{I(L)} \right] \quad (2)$$

σL is called the optical thickness or opacity, but in measurements of fire smoke the term optical density (D) has more commonly been used. Specifically

$$D = \log \left(\frac{I(0)}{I(L)} \right) \quad (3)$$

or

$$D = \sigma L / 2.303 \quad (4)$$

A measure of D , or more precisely σ , is not necessarily complete in order to define visibility. Here "visibility" will be more narrowly defined as L_v , the maximum distance which allows a visual discrimination of an object. A measure of visual discrimination has normally been based on an observer's ability to see an object or read a sign. It could more quantitatively be evaluated in terms of contrast levels and other optical parameters. As described so well by Jin [5], the visibility depends on the light intensity of the object, the intensity of the background and illuminating light, plus the scattering (σ_s) and absorption (σ_a) coefficients of the smoke. The total extinction coefficient σ is the sum

$$\sigma = \sigma_a + \sigma_s, \quad (5)$$

and thus σ alone does not provide sufficient information to predict visibility through smoke. Nevertheless, it has been shown by Jin [5] that for a back-lighted or illuminated sign, σL_v is approximately a constant which depends on the intensity of the light leaving the sign and the ratio of scattering to extinction coefficient for the smoke. Experimental results by Jin and others [1, 29] are given in Figure 1 (the data bars represent the spread of results due to different smokes). These data were based on observations of different objects by subjects whose eyes were protected from direct contact with the smoke; consequently, irritant effects have been eliminated. The scatter in the data represent the variations of light intensity from the viewed object and of the smoke optical properties. For fire safety design purposes the relationship σL_v or $(D/L) L_v = \text{constant}$ could be used by selection of an appropriate "design constant" (k_v) from Figure 1. By measuring optical density per path length (D/L) for smoke generated by a particular material, the maximum distance for vision is determined by

$$L_v = \frac{k_v}{(D/L)} \quad (6)$$

MACROSCOPIC EQUATIONS FOR SMOKE AND OPTICAL DENSITY.

The optical density of smoke depends on the mass of suspended particles and on the optical properties of the smoke aerosol, and any attempts at correlating laboratory smoke tests of a material with its performance in full-scale fire experiments must be couched in terms of the conservation of mass for smoke. This equation will be derived, expressed in terms of (D/L) , and its various forms will be considered in applications to predicting or correlating smoke concentration or light transmission.

A macroscopic mass balance equation will be derived for a fixed finite control volume in which smoke is produced. In principle, the control volume could be shrunk to a point, and thereby the corresponding spatial differential equation could be derived. Figure 2 shows an arbitrary control volume bounded by walls with two openings, and within which is a fire or decomposing material of involved surface area, A .

The conservation equation of smoke (specifically, its particulate mass conservation for the fixed control volume) is given as

$$\frac{d}{dt} \iiint C_s dV + \iint C_s \bar{v} \cdot \bar{n} dS = \dot{m}_{s,\text{net}} \quad (7)$$

$$\left[\begin{array}{l} \text{Rate of accumulation} \\ \text{of smoke (particulate} \\ \text{mass) in the control} \\ \text{volume, } V \end{array} \right] + \left[\begin{array}{l} \text{Net rate of smoke} \\ \text{leaving the control} \\ \text{volume through surface} \\ S \end{array} \right] = \left[\begin{array}{l} \text{Net rate of} \\ \text{smoke pro-} \\ \text{duced} \end{array} \right]$$

where C_s is the mass of particulates per unit gas volume

\bar{V} is the velocity of the aerosol (assumes the particles move with the bulk gas velocity)

and \bar{n} is the unit, positive outward, surface normal vector.

The net rate of smoke produced is

$$\dot{m}_{s,net} = \dot{m}_s - \dot{m}_{s,lost} \quad (8)$$

where the rate of smoke generated (\dot{m}_s) is expressed in terms of a fraction of particulate mass to total mass loss (smoke fraction), χ , where

$$\chi = \frac{dm_s}{dm} \quad (9a)$$

and m is total mass lost. For a fire fully involving a fixed area, A ,

$$\dot{m}_s = \chi \dot{m}'' A. \quad (9b)$$

This case will be considered for simplicity in the following development.

The rate of smoke lost, $\dot{m}_{s,lost}$, depends on particulate settling, adhesion to the solid surfaces, and volatilization of the particulates. Condensation of species to form more liquid particulates is also possible. These processes will not be addressed in further detail, but bear on appraising the accuracy of smoke correlations. Since no accounting of these losses is taken in any of the studies on fire smoke performed, a full quantitative accounting of its effect can not be presented. It is present in all systems, but its effect has been ignored in analyses of smoke production.

Since light transmission is the convenient form of smoke measurement, Equation (7) is more appropriately expressed in terms of optical density. This is easily done since experimental results and electromagnetic theory [6-9] give

$$\sigma_a = k_a C_s / \rho_s \quad (10a)$$

and

$$\sigma_s = k_s C_s / \rho_s \quad (10b)$$

where ρ_s is the density of the smoke particulate and the parameters k_a and k_s depend on wavelength (λ), particle size and shape and index of refraction.

For smoke composed mainly of soot (an absorbing and scattering aerosol), the scattering component is negligible in the visible range [7] and

$$\sigma \sim \sigma_a = k'_a C_s / (\rho_s \lambda^{1.39}). \quad (11)$$

"White" smoke or smoke generated from smoldering or non-flaming thermal decomposition tends to be primarily a scattering medium in the visible range [10].

Seader and Ou [11] have found a very useful result for both flaming and non-flaming radiative decomposition at 2.5 W/cm^2 for a number of materials and even for combinations of materials [12]. They show that at the completion of the decomposition process

$$(D/L) = \alpha C_s, \quad (12)$$

where $\alpha = 1900 \text{ m}^2/\text{kg}$ for non-flaming and $\alpha = 3300 \text{ m}^2/\text{kg}$ for flaming decomposition. The results are consistent with electromagnetic theory calculations [11] and the data of others [13, 14]. But the dependence of α on time, heat flux, and initial smoke concentration is not fully resolved. Yet Equations (10) and (12) can provide extremely useful results in generalizing our understanding of smoke from fire.

The parameter α in Eq. (12) has been termed the "particle optical density" by Seader and co-workers. It could also be termed a specific extinction coefficient (per particulate volume fraction) as suggested by Eq. (10). Equation (12) will be used to introduce optical density into the mass balance equation for smoke. Hence from Eqs. (7), (9b) and (12):

$$\frac{d}{dt} \iiint \frac{1}{\alpha} \frac{D}{L} dV + \iint \frac{1}{\alpha} \frac{D}{L} \bar{v} \cdot \bar{n} dS = \dot{\chi} m'' A - \dot{m}_{s, \text{lost}} \quad (13)$$

This is the basic equation that must be used to predict or correlate light transmission data for smoke.

Assuming no losses, the mass rate of smoke particulates produced can be calculated by the left-hand-side of Eq. (13); other than α , these parameters are typically measured in fire tests. The total (net) mass of particulates produced over time t (assuming no losses) is

$$m_s = \iiint \frac{1}{\alpha} \frac{D}{L} dV + \int_0^t \iint \frac{1}{\alpha} \frac{D}{L} \bar{v} \cdot \bar{n} dS dt \quad (14)$$

Without the α factor this has usually been called "total smoke" or some similar term. A related term is the specific optical density, D_s , as introduced by Gross et al. [15], but defined in a more general sense here as

$$D_s = \left[\iiint \frac{D}{L} dV + \int_0^t \iint \frac{D}{L} \bar{v} \cdot \bar{n} dS dt \right] / A. \quad (15)$$

The specific optical density is the optical density, D , per unit pathlength, L , resulting from the decomposition over a material's surface area, A , times the volume, V , of smoke produced in time t . For a closed uniform system, such as the smoke density chamber (SDC) [15, 47],

$$D_s = \frac{DV}{LA} \quad (16)$$

Alternatively, for α independent of time (and space) or taken as a suitable mean value,

$$D_s = \alpha m_s / A \quad (17a)$$

or

$$D_s = \alpha \chi m'' \quad (17b)$$

if χ is also assumed independent of time and where m'' is the material mass lost per unit area in time, t . The product $\alpha\chi$ has been referred to as the "mass optical density" by Seader and others. It has been suggested as a more fundamental index of smoke than D_s , since D_s is dependent on material density and thickness while $\alpha\chi$ is not [16]. This appears to have some advantage in evaluating a homogeneous material of varying thickness.

Separately, the parameters α and χ represent "smoke or fire properties" of a material. The α is related to fundamental parameters through electromagnetic theory and hence depends on wavelength, index of refraction and particle size. Although not a fundamental property, it is a useful engineering parameter in predicting light transmission in smoke. The mass fraction of smoke, χ , is more complex and relates to the mechanisms involved in thermal decomposition and smoke (soot) formation in flames. These parameters need to be examined more fully to be able to utilize Eq. (13) to predict or correlate smoke transmission. Their dependence on time and environment for a material needs to be known in order to generalize test results to arbitrary fire conditions. With these considerations in mind, correlations or predictions can and have been made, but they are undoubtedly based on insufficient information. This will be illustrated in the correlation results to be presented.

Equations (15) and (17) provide the basis for scaling and correlation of smoke measurements. It is assumed that *under the same conditions of heating, environment composition, and velocity, a given material decomposing uniformly (or similarly) over a fixed area and orientation will have an invariant D_s at a given time.* This follows from Eq. (17a), provided smoke losses per unit area A are negligible or $(m_{s,lost}/m_s)$ is invariant. This means that for any fire system described by the control volume equation ((13) or (14)), D_s as evaluated by Eq. (15) should be equal for two different systems (e.g. test method and full-scale) provided the restrictions of the assumption are met. For a control volume which always encloses the smoke (even the smoke flowing out of the test chamber), i.e. a closed system, it can be shown that for α and χ independent of time:

$$\frac{1}{\alpha \dot{m}''} \frac{dD_s}{dt}_{\text{closed system}} = 1 - \frac{\dot{m}_{s, \text{lost}}}{\dot{m}'' A} \quad (18a)$$

or integrated over time,

$$D_s(t) = \alpha \chi m'', - m_{s, \text{lost}}/A \quad (18b)$$

Hence, *the mass optical density of two systems will be equal if their D_s values are equal.* Again, losses must be negligible or similar and the area involved must be well defined. The application to a spreading fire under varying heating and environmental conditions presents difficulty!

Within the limits noted above, two special cases will conveniently serve as a basis in our discussion and development of correlations.

CLOSED SYSTEM. The first is a closed system uniformly mixed with no smoke losses:

$$\frac{dD_s}{dt} = \alpha \dot{m}'' \quad (19a)$$

or

$$D_s = \alpha \chi m'' \quad (19b)$$

where

$$D_s = \frac{DV}{LA}$$

V being the volume of the system.

STEADY OPEN SYSTEM. The second case is the steady flow open system with air entering and smoke leaving, with no losses:

$$\alpha \chi = \frac{D}{L} \frac{\dot{V}}{\dot{m}'' A} \quad (20a)$$

where \dot{V} is the volume flow rate of smoke leaving the system, or

$$D_s = \alpha \chi m'' = \int_0^t \left(\frac{D}{L} \right) \dot{V} dt / A \quad (20b)$$

From light transmission measurements in the smoke and flow measurements, it is then possible to determine $\alpha \chi$ or D_s for these systems. If the decomposed area is well-defined then D_s is the appropriate correlating parameter; if mass loss is measured then $\alpha \chi$ is the appropriate parameter. The use of either involves the assumption of time independence for α and χ , and also that negligible or similar smoke losses occur.

FACTORS AFFECTING SMOKE PROPERTIES: D_s , α , χ .

The parameters α and χ can be considered "bulk" material properties, although D_s cannot; it is a dimensionless optical density. In analogy to the heating of a solid, D_s is to dimensionless temperature as $\alpha\chi$ is to the thermal parameter $k\rho c$. Yet α and χ are not to be taken as fundamental properties, such as the density of a pure substance; they are more like bulk density of an aggregate. In addition α and χ must depend on both solid and gas phase phenomena, i.e. decomposition, the flame dynamics, and its chemistry. Based on the results of many investigators, factors affecting $\alpha\chi$ as well as D_s can be identified. Reported values for D_s were related to the product $\alpha\chi$ through Eq. (17b) but no attempt was made to assess α and χ independently. Thus a full characterization of the smoke properties of a material has not been done, but a sense of the dependent variables can be inferred from the results reported for D_s and $\alpha\chi$. An excellent review on fire smokes and a discussion of factors affecting D_s and $\alpha\chi$ was reported by Seader and Einhorn (17). The qualitative effect of these factors will be discussed.

TIME. The quantity D_s will increase with time as the material decomposes, reach a maximum, and then tend to slowly decrease as smoke losses dominate smoke production [15] (e.g. see Eq. (18b)). The mass optical density, $\alpha\chi$, as derived from Eq. (17b) is also found to have a similar behavior in time. However, lack of data acquisition synchronization between measurements of sample mass loss and optical density (or light transmission) as well as the effects of non-uniform smoke concentration could have affected the time response for $\alpha\chi$ [18]. Moreover α has only been measured at the end of decomposition (not over time), and only at a fixed radiant heating level, 2.5 W/cm^2 [11-13]. It is significant to note that the calculation of $\alpha\chi$ by Eq. (17b) assumes α and χ are independent of time, yet experimental results demonstrate otherwise; hence, a "time-averaged" value for $\alpha\chi$ is presented. Until α and χ are measured individually over time, a clear understanding of their time behavior during decomposition is not possible.

EXTERNAL RADIANT HEAT FLUX. Many investigators have demonstrated the dependence of D_s and $\alpha\chi$ on external radiant heat flux for both flaming and non-flaming [1, 14, 18-23]. The non-flaming mode is arrived at by not using a pilot flame; however, at high heat fluxes auto-ignition may occur and therefore a strictly non-flaming or "smoldering" decomposition may not be possible (except in an inert atmosphere). Thus at high flux levels a non-piloted result does not necessarily mean non-flaming. Lack of clarity or completeness of such results found in the literature leaves the data ambiguous. Usually there appears to be an increase of $D_{s, \max}$ with flux but this is not true for all materials. The results of Brown [23] show a dramatic increase in $D_{s, \max}$ between 2.5 and 5.7 W/cm^2 for non-piloted ignition. While this could be due to auto-ignition, it is not explicitly stated. For these materials the non-piloted irradiances produced higher values for $D_{s, \max}$ than their piloted counterpart. In these studies a vertical

sample orientation was used so that melting of materials would affect the result, and a poorly defined decomposition area affects the calculation of D_s . Since mass loss is also dependent on heat flux it is not clear from D_s data alone how $\alpha\chi$ depends of flux. Since $\alpha\chi$ generally is a more useful result, an example of the dependence of $\alpha\chi$ on flux is shown in Figure 3. These results were derived for the piloted data presented by Brown [23]. The $\alpha\chi$ was calculated using Eq. (19b) at the peak value of D_s or where the final data on mass loss were available. These results clearly show that the dependence of flux on $\alpha\chi$ is significant, but even a qualitative trend cannot be drawn. More importantly the ranking of materials from low to high $D_{s,max}$ values changes significantly between the low (2.5 W/cm²) and high (11.3 W/cm²) flux levels in the piloted and non-piloted data of Brown [23] as seen for the piloted data in Figure 4.

TEMPERATURE. Temperature of the environment could be viewed as a surrogate for radiant heat flux. This is especially so if the heated gas is confined in a room or test oven. Hence a similar effect would be expected. Indeed, studies by Saito [24, 25] and Tsuchiya and Sumi [26] and more recently by Bankston, *et al.* [27] show a distinct but not generally similar relationship for all materials. For example, Saito [24, 25] finds that $\alpha\chi$ both can increase or decrease linearly with temperature under either non-flaming or flaming conditions; similar to the results for flux in Figure 3.

OXYGEN CONCENTRATION. The effect of environmental composition has not been studied extensively, but limited results by Gross, *et al.* [15] (non-flaming) and King [13] (flaming) tend to show a decrease in $D_{s,max}$ as oxygen concentration is decreased. In contrast, Saito [24] finds that in compartment fires $\alpha\chi$ decreases rapidly as the compartment ventilation parameter ($A\sqrt{H}$) is increased, then tends to level off for "large" $A\sqrt{H}$. The "large" $A\sqrt{H}$ behavior Saito finds is consistent with his temperature dependence for $\alpha\chi$ predicted from his test data. For compartment fires it can be inferred that at low $A\sqrt{H}$ values the decomposition is occurring in a low oxygen concentration environment. Thus Saito's compartment fire data imply that $\alpha\chi$ increases as oxygen concentration is decreased, i.e. $\alpha\chi \uparrow$ as $A\sqrt{H} \downarrow$ and $O_2 \downarrow$ as $A\sqrt{H} \downarrow$. This result for ventilation controlled compartment fires could be consistent with the observation that D_s decreases as oxygen decreases [13, 15] since $D_s = \alpha\chi m''$, Eq. (17b).^s Then as $A\sqrt{H} \downarrow$, $O_2 \downarrow$ and $m'' \downarrow$ (for ventilation controlled fires), $D_s \uparrow$ as $\alpha\chi \uparrow$ provided the decrease in m'' is weak. Hence, here is another example where the need to separate effects on α , χ , and m'' is apparent.

SCALE. Not much work has been done to investigate the effect of scale on smoke production. In particular the sample size has not been varied without varying the scale of the entire system. Two experiments using the smoke density chamber and a large closed compartment yield inconclusive results: the data of Lopez [1] suggest a tendency for $D_{s,mass}$ to decrease as the sample area is increased ($s \times s$ vertical sample where $s = 0.02, 0.09, 0.18, 9.27$), but the results of Shores [32] show no distinct trend. It

is expected since D_s depends on mass loss per unit area, \dot{m}'' , that there is bound to be an effect of scale of D_s . The dependence of \dot{m}'' on scale will vary as flow conditions vary from laminar to turbulent and as flame heat transfer changes with flame size and shape. However understanding the effects of scale on the components of D_s : α , χ , and \dot{m}'' would be more revealing.

ORIENTATION. Some factors that relate to scale also apply to orientation namely, the fluid and heat transfer effects caused by the flame and other heat sources. In addition, the melting and structural erosion of a material due to its orientation can have a significant effect on the smoke measurement. For example, Breden and Meisters [28] found that $D_{s,max}$ is much greater for a horizontal melting sample than a vertically mounted sample in the smoke density chamber. Yet similar values for $D_{s,max}$ were measured in both orientations for nonmelting specimens, but dD_s/dt up to $D_{s,max}$ was greater for the horizontal case. These results suggest that melting results in an unspecified heated area, and differences in flame configuration affect the rate of smoke production more than the total smoke produced.

MODE OF DECOMPOSITION. It is apparent that the intensity and manner of thermal decomposition affects the amount and nature of the smoke particulates generated. Foster [10] finds the smoke produced from non-flaming thermal decomposition of wood saw-dust consists of spherical droplets of nearly pure scattering character, while King [13] finds, under flaming decomposition, that smoke can be composed of chainlike elements of both solid and liquid particles. Jin [5] reports similar findings with non-flaming thermal decomposition giving particles of less than 1 μm in diameter (white smoke); but for flaming, (black smoke) particle size ranges up to 20 μm .

Another effect of scale, not considered earlier, relates to the destruction of smoke particles by their evaporation and oxidation as they traverse the flame and plume. The nature of the particulates -- liquid drops, carbon soot, "chains" -- at their origin would surely affect this process. Hence "big" flames may not be similar to "small" flames in their net production of smoke particulates which emerge from the flame zone.

THICKNESS AND DENSITY. It has been reported by several investigators [17] that $D_{s,max}$ depends nearly linearly on sample thickness up to some thickness after which it approaches a constant. A similar behavior is claimed for initial sample density [17]. This effect is mainly due to mass lost (\dot{m}'') in correspondence to $D_{s,max}$ since that mass is dependent on density and thickness. In contrast, it is found that $\alpha\chi$ is much less dependent on sample thickness and density [16].

CONCLUDING REMARKS. Although other parameters may be relevant variables for smoke production, the above set appear to be the most significant. Despite the identification of these parameters it is not clear what the most fundamental set of variables describing smoke are or what other variables they depend on. Both D and the mass optical density ($\alpha\chi$) are composed of several parameters, each of which depend on other variables. Heat flux is a dominant and convenient independent variable for representing smoke "properties" but it does not constitute a fundamental variable. Heat flux promotes decomposition which produces smoke, (but it is the ultimate temperature of the material and its time varying state on which the rate of decomposition depends). Also smoke fraction, χ , represents the result of a series of processes: solid degradation, nucleation of particulates, growth and decay in the flame, coagulation, and vaporization. Nevertheless, it is useful to represent χ as a function of heat flux for a given material for engineering calculations. Further research needs to establish valid limitations to such functional relationships for this approach to be sound.

Additional information on factors controlling smoke production can be found in an extensive review by Seader and Einhorn [17]. Also the papers by Rasbash, et al. [29, 30] are interesting general articles on smoke.

COMPARISONS BETWEEN TEST (METHOD) DATA AND LARGE SCALE FIRE EXPERIMENTS

The ground work has been laid for establishing a basis for correlating results of test data and fire measurements. Also the factors affecting these results have been discussed. A well defined test method environment (e.g. heat flux) helps to yield a specific smoke property; yet, this result may be insufficient for application to a large scale fire. The environment of a large-scale fire is complex, not sufficiently predictable, and not completely measurable. For example, the heat flux from the flame of a burning object, and additional convective and radiative heating from a hot enclosure will not necessarily be equal to the prescribed radiative heat flux in the test method. Moreover, test methods subjectively intended to simulate conditions in a realistic fire generally have no scientific basis nor have they universal application. This dilemma has been further elaborated on by Robertson [31].

With these considerations realized, available and derived results will be presented for comparison. An attempt was made to provide homogeneity in the comparisons; meaning, results were presented in terms of D or $\alpha\chi$ as established from the governing equations. When insufficient information did not allow this format, appropriate "related" parameters were compared.

COMPARISONS FOR CLOSED SYSTEMS.

Several investigators [1, 32, 33] have examined results from the smoke density chamber* (a closed system) with scaled-up versions of irradiated samples burning or decomposing (non-flaming) in a large chamber. Lopez [1] varied both the flux and sample size, Shores [32] varied the sample size maintaining the prescribed test flux of 2.5 W/cm^2 , and Robertson [33] reports results for the NBS chamber sample producing smoke in an 18 m^3 room. The results of the full-scale data are compared with the standard smoke density chamber findings in terms of $D_{s,\text{max}}$ (Figure 5). Shores [32] also displays comparisons continuously over time of comparable agreement as those discrete data shown in Figure 5. If the smoke losses are similar or negligible in both systems, and sample scale effects (vertical orientation) are small, then the $D_{s,\text{max}}$ results should be identical. The variations from that ideal are shown in Figure 5.

COMPARISONS WITH FULL-SCALE ROOM FIRE GROWTH DATA.

A variety of materials and fuel configurations were burned in rooms in which the optical density of the smoke leaving the system was measured. Correspondingly, small-scale laboratory test data were taken for the materials, and comparison could then be made with the full-scale results. In some cases these comparisons were explicitly reported in the literature, in other cases they were derived from reported data. The first set of data compared are in terms of homogeneous parameters: $D_{s,\text{max}}$ or $\alpha\chi$. The sources [34-41] of these data, their full-scale test configurations, the test method used for the material, and a tabulation of the results are given in the Appendix. Six sets of comparisons are plotted in Figure 6. The range of configurations includes random arrays [34], wall linings [35, 41], mattresses (horizontal and vertical) [36-39], and small tables [40]. The materials include plastics, wood, cotton, rubber, painted surfaces, and others (See Appendix). The methods for calculating the $D_{s,\text{max}}$ or $\alpha\chi$ values for the fullscale experiments are based on Equations (19) and (20). The specific form of the equation used is indicated in Appendix B. As it might be expected, a direct correlation does not result. Nevertheless, there is a general trend in the proper direction implying, except for a few out-lying data points, that uncontrolled influencing variables do not have a very strong effect. The effect of material configuration is very strong as indicated by the data (Appendix) given for polystyrene, e.g. its coordinates range as follows:

$$\alpha\chi = (700, 180), (1000, 785), (820, 790);$$

$$D_{s,\text{max}} = (3.8, 43), (63, 32).$$

* Brief descriptions of test methods or laboratory based procedures listed in the Appendix.

Since no assessment of accuracy could be made in these experiments, these differences must be regarded as solely due to fuel arrangement and material configuration. Whether $\alpha\chi$ or $D_{s,max}$ is selected as the correlating variable has no apparent advantage in these comparisons. The underlying complexities present in these processes can be illustrated from a study by Saito [24]. He presents $\alpha\chi$ as a function of compartment temperature and ventilation factor ($A\sqrt{H}/A$) in Figure 7. His laboratory test data, derived from using a furnace to decompose materials at a fixed temperature, correlate well with small and large scale compartment room lining fires except below compartment temperatures of 700°. This low temperature range corresponds to small compartment openings (small $A\sqrt{H}$) in which reduced oxygen concentration tends to increase $\alpha\chi$. Since the effect of oxygen is not measured in the test data, its influence on the compartment data is not accounted for.

Another illustration of the limits of simple correlation procedures is given from the work of Tustin [21]. The OSU combustibility apparatus was used to determine $D_{s,max}$ at 1.5, 2.5, 3.5 and 5.0 W/cm² irradiances. Full-scale results were derived from burning 2.1 m² of material for two simulation conditions under varied external radiation of up to 8.9 W/cm² in a ventilated Boeing 707 aircraft section. The results shown in Figure 8 leaves to question the selection of an unambiguous test heat flux.

Now a series of comparisons will be presented in which "nonhomogeneous" smoke parameters were used. In most cases the parameters are related to $\alpha\chi$ or D_s , in other cases the relationship must be regarded as empirical. Christian and Waterman [42] conducted a series of full-scale room and corridor fires in which lining materials were ignited by gas burner exposure fires. The full-scale results were expressed as

$$Y = \int_0^t \left[(D/L) - (D/L)_{\text{burner fire}} \right] dt$$

(in which the exposure fire smoke was considered). Y is proportional to a D_s since their gases were exhausted at a constant volume flow rate. They compared these results to a variety of test apparatus measurements including the ASTM E84 Steiner tunnel test method, but with its smoke results given as

$$X = \int_0^t (D/L) dt$$

instead of its standard classification form. They concluded that the smoke density chamber test in a non-piloted mode gives best results for fully involved lining fires in a room as seen in Figure 9. However the tunnel test appeared best for spreading fires in a corridor as illustrated in Figure 10. These illustrations show only a portion of their available

data [42], but were selected as illustrations most consistent with their conclusions. Fang's result [43] tend to support the tendency of the smoke density chamber non-flaming data to correlate the results for lining fires in a room (Figure 11). The tunnel classification correlation, in which the (upper) abscissa

$$X = 100 \int_0^t (1-I/I_0)dt / \int_0^t (1-I/I_0)dt, \text{ red oak}$$

appears to yield results of similar character. The tunnel correlation is entirely empirical, but the comparison with the smoke density chamber could have been in terms of D_s if the ordinate in Figure 11 was divided by the area burned in each case. This information was not reported.

Although the results of Babrauskas [37-39] are shown in Figure 6, these were derived from his data not computed by him. He advocates [39] the use of $\alpha\chi$, but instead he presented a correlation which attempts to incorporate a fire growth effect for the mattress fire scenario studied [38]. In that study the full-scale parameter

$$Y = \sigma_{\max}$$

is plotted against the laboratory test parameter $X = (\alpha\chi)E$ where E is the rate of energy release averaged over three minutes as derived from the NBS II calorimeter or the OSU combustibility apparatus. This empirical correlation gives results generally similar to those plotted in Figure 6 for the same experiments.

Finally results were replotted from Moulen, et al. [44] on linear coordinates rather than logarithmic coordinates as used by them. They burned lining materials in a room's corner subject to a wood crib fire or by radiant exposure using the heat source provided in the laboratory Early Fire Hazard (EFH) test used in Australia. These variables compared were

$$Y = \frac{1}{\Delta t} \int_{t_f}^{t_f + \Delta t} (D/L)dt$$

and

$$X = \frac{1}{\Delta t} \int_{t_p}^{t_p + \Delta t} (D/L)dt$$

where $\Delta t = 1$ minute, t_f is the time flames touched the ceiling of the room, and t_p is the time when D reached a maximum. These results are shown in Figure 12.

Individual judgement is undoubtedly used in deciding the merits of these various correlations. Although empirical results may seem to be positive at times, it is nearly impossible to generalize these results with confidence. The overwhelming effect of these comparisons raises more questions than gives answers.

COMPARISONS BETWEEN TEST METHODS.

Since various test methods and modifications thereof have been used to measure the smoke production of a material, it is useful to compare parameters measured in test methods. Under controlled conditions, a smoke property for a material should be independent of the apparatus that was used to measure it. It should only depend on the factors listed previously (i.e. heat flux, scale, etc.)

It was reported by Gross, et al. [15] that the ASTM E-84 Tunnel classification and the smoke density chamber (SDC) in a non-flaming mode did tend to correlate, but the correlation was poor for the flaming mode. This unexplainable result is consistent with those data presented in Figures 9 and 11. It might be speculated that the tunnel test fire is like a fully-developed, ventilation-limited, fire which has an excess of unburned fuel and particulates as would be the case in non-flaming radiative decomposition. Only a thorough study of these phenomena could unravel the mechanisms producing these results.

In Figure 13, results are compared from the OSU apparatus with the SDC at 2.5 and 5.0 W/cm² in a flaming mode [21]. Also both flaming and non-flaming SDC results are compared with smoke collected in a 18 m³ closed room as a result of the British fire propagation test [33]. The comparison between SDC and OSU should be identical unless measurement uncertainties are present. The comparison with the British smoke test agrees best for the non-flaming SDC data. Again, the British fire propagation test very likely is ventilation limited, and perhaps produces "unburned" smoke as in non-flaming decomposition. Finally, recent studies by Hilado, et al. [45] compare data for wood and plastic materials using the SDC and the Arapahoe smoke test. The Arapahoe device exposes a small sample to a (propane) flame for 30 seconds collecting the particulates on a filter over that 30s period and for an additional 30s while the burner flame is off. Thus, the heat flux and local environment are not clearly defined and flaming or non-flaming decomposition occurs over some portion of the material. The SDC tests were conducted at the standard conditions but they presented average results from tests using two different pilot burners. A correlation is perceived by the authors [45] but not explained and seems dubious at low "Arapahoe values". The correlating parameters are $D_{s,max}$ (SDC) and m_s/m_o (Arapahoe) where m_o is the initial sample mass. If conditions were similar in the two tests, then for the same sample thickness and material it follows from Eq. (17) that

$$D_{s,max} = \alpha m_s/A = \alpha(\rho\delta) (m_s/m_o)$$

where ρ is the initial sample density and δ is its thickness. Thus if α is a constant for all materials (which appears so in flaming or non-flaming decomposition), the $D_{s,max}$ as determined by the SDC should correlate with (m_s/m_o) but only if the same conditions of heat flux and pilot exposure prevail. This is not the case in the Arapahoe system, and hence the correlation is only justified in principle, but not necessarily by their [45] data. Ou and Seader [46], using a modified SDC at 2.5 W/cm^2 with mass monitoring and an Arapahoe Chemical Company Smoke Chamber with a modified downward burner flame exposure of 45 s, did demonstrate a reasonable correlation. It was couched in terms of

$$\left(\frac{D}{L}\right)_{\text{SDC}} \text{ vs } (\chi)_{\text{Arapahoe}} \left(\frac{m}{V}\right)_{\text{SDC}}$$

which follows from Eq. (17b). Differences in heat flux conditions must still be considered and must bear on these results as well.

CONCLUSIONS

This review has attempted to demonstrate how smoke measurements have been used to evaluate a material's contribution to fire. These measurements primarily pertain to the light transmission characteristic of smoke and have a direct bearing on visibility. It was shown (Figure 1) that visibility in smoke (L_v) is directly related to the optical density per unit path length (D/L), but further depends on lighting conditions and more specific smoke properties than are currently being measured. The design for visibility through smoke can be approximately carried out using existing data from current test methods, but more attention needs to be given this problem.

The governing equation for smoke (Eq. (13)) clearly shows the need to evaluate the parameters: α ("particle optical density") and χ (smoke particulate fraction) in order to predict the extinction (D/L) of light in smoke or smoke concentration. Currently the parameters most often used to characterize smoke have been (maximum) specific optical density $D_{s,max}$ and so-called "mass optical density", $\alpha\chi$. Although these two parameters may be convenient and fitting for most practical applications they are not necessarily sufficient or consistent with the requirements for calculating smoke concentration and extinction. D is an extensive parameter representing the accumulation of smoke over time, not its instantaneous production. The "lumped-parameter" $\alpha\chi$ is determined by operations which presume α or χ or both are time averaged values. Since significant changes occur over time, suitable time-averaged results consistent with the process of decomposition should be established. For example, smoke produced in the fully-developed fire state must be discriminated from smoke produced in the fire decay or charring state.

D_s or $\alpha\chi$ may still be useful representations for smoke, but their basis must be examined more closely relative to the decomposition process and the imposed environment. Research is required to develop apparatus and instrumentation to directly measure α and χ along with sample mass loss over the duration of decomposition. Provision should be made to examine the effect of environmental heat flux and oxygen concentration since these appear to have the greatest influence on smoke production. A "steady" flow-through device would be better than a closed system apparatus for measuring these smoke properties. This would allow wall losses to be minimized and smoke properties to be measured at the flame source. It could be argued, however, that "aged" smoke might be more appropriate to measure for fire considerations. The development of an accurate coagulation and wall loss model to predict the nature and concentration of smoke as it collects and flows away from a fire would eliminate this argument. Ideally both "early" and "long-time" smoke measurements should be pursued.

An important variable on which smoke production depends is the heat flux received by the material. In a test method this is usually only characterized by the applied external flux. In fact, it is composed of the flame heat flux and the external flux. In full-scale fires, the scale and orientation of the material establishes the flame heat flux, and the structural aspects of the environment control the additional "feedback" heat flux. Predictive techniques have not yet been developed to determine these various heat fluxes from basic principles, particularly when radiative components are present. Until the predictions are possible, well conceived full-scale experiments designed to measure these heat fluxes could be conducted. The availability of material data for smoke in terms of parameters like α , χ , \dot{m} and their dependence on applied (or total) incident heat flux would establish a basis for a prediction. A demonstration of this correlation procedure, more general than the "scaling" results of Figure 5, is needed as a step in establishing the credibility or deficiencies of this process. The alternatives are to rely on short-cut correlations, such as $D_{s,max}$ at 2.5 W/cm^2 versus $D_{s,max}$ derived in full-scale; or to use empirical procedures and test methods, such as the Steiner tunnel which looks like a "big" fire and rates materials relative to red oak.

Although practical applications may have to be simply executed, they can not be soundly arrived at through incomplete information. Test apparatuses should not be regarded as unique sources of information; it is the smoke property measured for the material that should be established as unique. As can be seen by the data presented in this review, correlations between test methods and full-scale fire data depart as the full-scale fire becomes more complex. Fire spread and ventilation limited conditions, usually found after full-involvement of the fuel in an enclosure, have a direct bearing on the smoke production. The conclusion from

these data reflects the futility of seeking correlations without a full understanding of the processes. The ability to make fine discriminations for material decomposition and exposure conditions in real fires does not exist. But the best use of available test methods could be utilized for the present. To be more relevant they may have to be tailored to more accurately match the fire scenario being considered. For example, in the post crash aircraft fire scenario in which the threat is a large fuel spill fire and safe egress is only viable before cabin flashover, the pre-flashover exposure heat flux and environmental conditions could be used to establish test method levels. These heat fluxes are high and both non-flaming (nonpiloted) and flaming smoke measurements need to be considered. Also fire spread and gas movement would have to be known or predicted for a complete analysis. Similar approaches have been already attempted and limited success has been achieved [21, 22]. More general modeling techniques are also possible but their ability to correctly predict fire spread is essential (e.g. [3]). If the test method data is available in a complete and consistent form for mathematical analysis it could be utilized in relationship to well-developed fire scenario test measurements and/or predictive models for that scenario. Then relevant correlations or predictions could be achieved.

REFERENCES

1. Lopez, E.L.: J. Fire Flammability, 6, 405 (1975).
2. Alarie, Y., Kane, L. and Barrow, C.: Sensory Irritation: The Use of an Animal Model to Establish Acceptable Exposure to Airborne Chemical Irritants in Toxicology: Principles and Practice, 1, ed. A.L. Reeves, John Wiley (1980).
3. MacArthur, C.D. and Meyers, J.F.: Dayton Aircraft Cabin Fire Model, Fed. Aviation Admin. Report, FAA-RD-76-120, I, II, and III (1978).
4. Howell, J.R. and Siegel, R.: Thermal Radiation, III, Nat. Aero. and Space Admin., NASA SP-164, 13 (1969).
5. Jin, T: Visibility through Fire Smoke (Part 2), Report of the Fire Research Institute of Japan, No. 33, 31 (1971).
6. Hottel, H.C. and Sarofim, A.F.: Radiative Heat Transfer, McGraw - Hill, N.Y. (1967).
7. Howell and Siegel, op. cit., III, 333-8.
8. Kerker, M.: The Scattering of Light and Other Electromagnetic Radiation, Academic Press, N.Y., (1969).
9. Bromberg, K. and Quintiere, J.G.: Radiative Heat Transfer from Products of Combustion in Building Corridor Fires, Nat. Bur. Stand., NBSIR 74-596, (1975).
10. Foster, W.W.: British J. Appl. Phys., 10, 416 (1959).
11. Seader, J.D. and Ou, S.S.: Fire Research, 1, 3, (1977).
12. Ou, S.S. and Seader, J.D.: J. Fire Flammability, 9, 30 (1978).
13. King, T.Y.: Smoke and Carbon Monoxide Formation from Materials Tested in the Smoke Density Chamber, Nat. Bur. Stand. NBSIR 75-901, (1975).
14. Chien, W.P. and Seader, J.D.: Fire Technol., 10, 187, (1974).
15. Gross, D., Loftus, J.J. and Robertson, A.F.: Methods of Measuring Smoke from Burning Materials, Amer. Soc. Testing and Materials, ASTM STP 422, 166 (1967).
16. Seader, J.D. and Chien, W.P.: J. Fire Flammability, 5, 151, (1974).
17. Seader, J.D. and Einhorn, I.N.: Some Physical, Chemical, Toxicological, and Physiological Aspects of Fire Smokes, 16th Symp. (Int.) on Combustion, The Combustion Institute, 1423, (1977).

18. Seader, J.D. and Chien, W.P.: Factors Affecting Smoke Development and Measurement, Univ. of Utah Report, FRC/UU 17a, UTEC-MSE 74-031 (Mar. 1974).
19. Gaskill, J.R., Taylor, R.D., Ford Jr., H.W. and Miller, H.H.: J. Fire Flammability, 8, 160, (1977).
20. Bankston, C.P., Cassanova, R.A., Powell, E.A. and Zinn, B.T.: J. Fire Flammability, 7, 165, (1976).
21. Tustin, E.A.: Development of Fire Test Methods for Airplane Interior Materials, Boeing Commercial Airplane Co., NASA Contract No. NAS9-15168 Final Rept. NASA CR-14568, (1978).
22. Spieth, H.H., Gamme, J.G. Luoto, R. E. and Klinck, D.M.: Investigate A Combined Hazard Index Methodology for Ranking an Aircraft Cabin Interior Material for Combustion Hazards, Part 1 - Final Rept. Draft, McDonnell Douglas Corp., DOT, Fed. Aviation Admin. (1981).
23. Brown, Jr. L.J.: Smoke Emissions from Aircraft Interior Materials at Elevated Heat Flux Levels using Modified NBS Smoke Chamber, Fed. Aviation Admin. Rept. No. FAA-RD-79-26, (1979).
24. Saito, F.: Smoke Generation from Building Materials, 15th Symp. (Int.) on Combustion, The Combustion Institute, 269, (1974).
25. Saito, F.: Smoke Generation from Organic Materials, Main Reports on Production Movement and Control of Smoke in Buildings, Occasional Report of Japanese Assoc. Fire Science and Engineering No. 1, (1974).
26. Tsuchiya, Y. and Sumi, K.: J. Fire Flammability, 5, 64 (1974).
27. Powell, E.A., Bankson, C.P., Cassanova, R.A.: Fire and Materials, 15 (1979).
28. Breden, L.H. and Meisters, M.: J. Fire Flammability, (1976).
29. Rasbash, D.J.: Trans. J. Plastics Inst., 55 (Jan. 1967).
30. Rasbash, D.J. and Pratt, B.T.: Fire Safety J. 2, 23, (1979/80).
31. Robertson, A.F.: Standardization News, 3, 18 (1975).
32. Shores, N.H.: Some Predictive Aspects of NBS Smoke Chamber Examination of Combustible Materials, Armstrong Cork Co. Tech. Res. Rept., (Dec. 1975).
33. Robertson, A.F.: Fire Technol. 10, 282, (1974).
34. Heselden, A.J.M.: Fire Problems of Pedestrian Precincts Part 1: The Smoke Production of Various Materials, Fire Research Station, U.K., Fire Res. Note No. 856, (1971).
35. Watts, P.R.: The Assessment of Smoke Production by Building Materials in Fires, Part 4. Large Scale Tests with Wall Lining Materials, Fire Research Station, U.K., Fire Res. Note No. 1013, (1976).

36. Parker, W.J.: Comparison of the Fire Performance of Neoprene and Flame Retardant Polyurethane Mattresses, Nat. Bur. Stand., NBSIR 73-177, (1973).
37. Babrauskas, V.: Combustion of Mattresses Exposed to Flaming Ignition Sources Part I.: Full-Scale Tests and Hazard Analysis, Nat. Bur. Stand., NBSIR 77-1290, (1977).
38. Babrauskas, V.: Combustion of Mattresses Exposed to Flaming Ignition Sources Part II. Bench-Scale Tests and Recommended Standard Test, Nat. Bur. Stand., NBSIR 80-2186, (1980).
39. Babrauskas, V.: J. Fire Flammability, 12, 51, (1981).
40. Evans, D.D.: Analysis of Data from Room Fire Test of Parsons Tables and Comparison with Laboratory Test Methods for Ignition, Flame Spread, and Smoke Generation, Nat. Bur. Stand., NBSIR (in review).
41. Woolley, W.D., Raffery, M.M., Ames, S.A. and Murrell, J.V.: Fire Safety J., 2, 61 (1979/80).
42. Christian, W.J. and Waterman, T.E.: Fire Technology, 8, 332 (1971).
43. Fang, J.B.: Fire Buildings in A Room and the Role of Interior Finish Materials, Nat. Bur. Stand., NBS Tech. Note 879, (1975).
44. Moulen, A.W., Grubits, S.J. Martin, K.G. and Dowling, V.P.: Fire and Materials, 4, 165, (1980).
45. Hilado, C.J., Machado, A.M. and Murphy R.M.: J. Fire Flammability, 9, 459, (1978).
46. Ou, S.S. and Seader, J.D.: Fire Research, 1, 135; (1977/78).
47. Standard Test Method for Specific Optical Density of Smoke Generated by Solid Material, American Society of Testing and Materials, ASTM E-662-79, Standards 1980.
48. Proposed Test Method for Heat and Visible Smoke Release Rates for Materials, American Society for Testing and Materials, Book of Standards 1980, pp. 1382-1400.
49. Standard Test Method for Surface Burning Characteristics of Building Materials, American Society for Testing and Materials, ASTM E 84-80, Book of Standards 1980.
50. Kracklauer, J.J., Sparkes, C.J. and Legg, R.E.: Plastics Technology, 22, 46 (1976).
51. Fire Propagation Test for Materials, British Standard BS 476 part 6 (1968).
52. Methods for Fire Tests and Building Materials and Structures (AS 1530), Part 3, Test for Early Fire Hazard Properties of Materials, Standards Association of Australia, Sydney (1976).

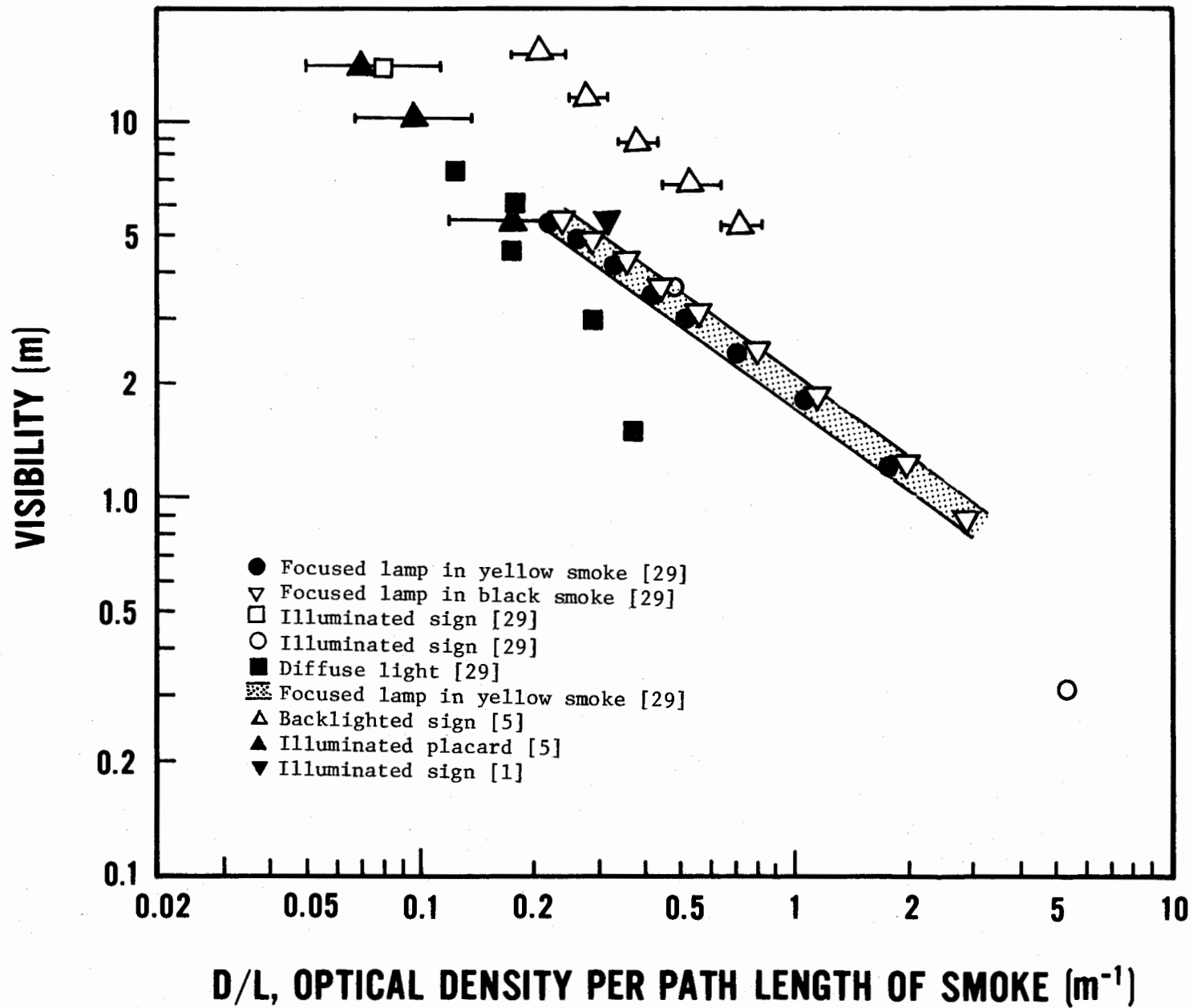


Figure 1 - Visibility Results Derived from Rashbash [29], Jin [5], and Lopez [1]

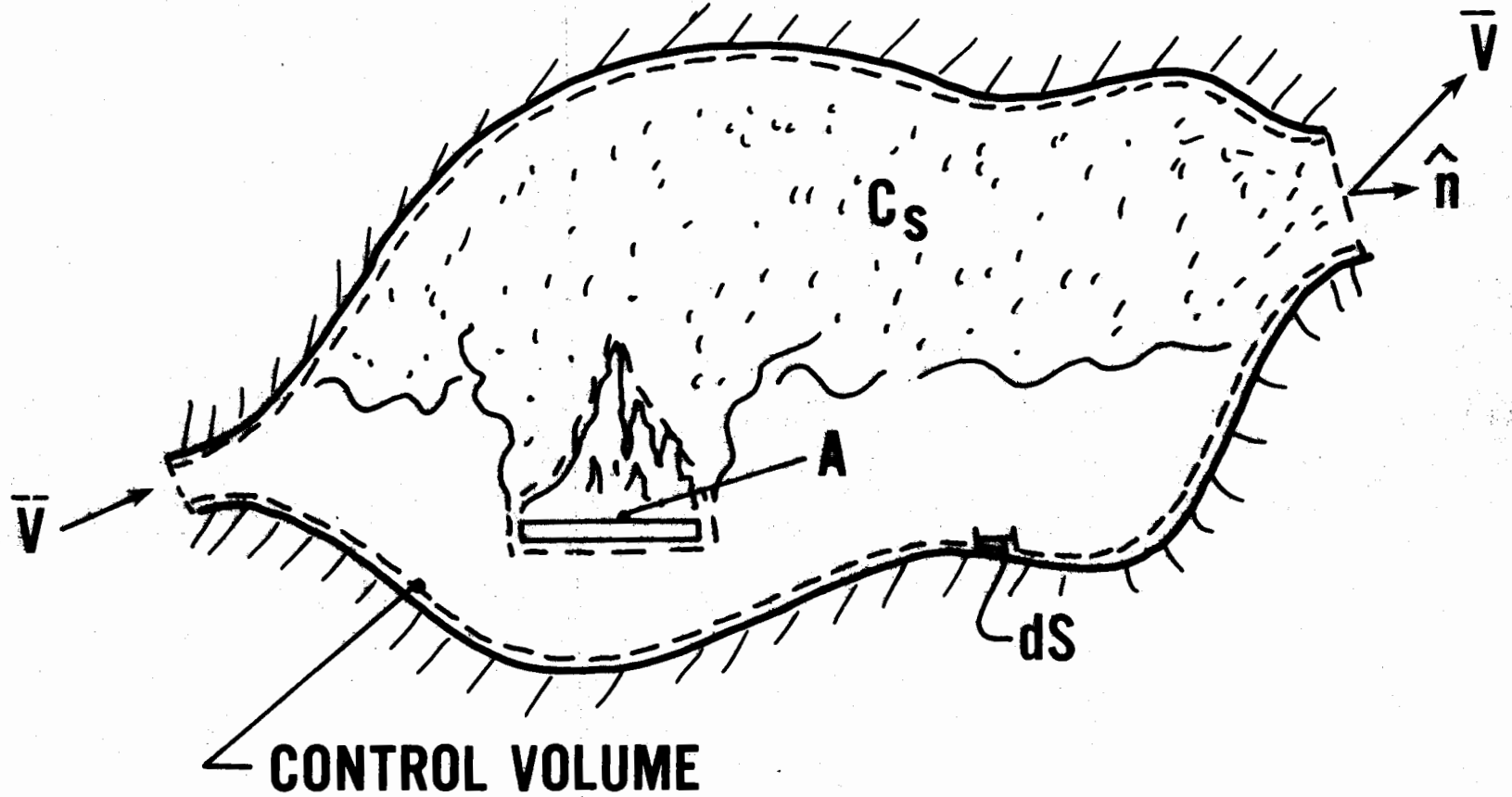


Figure 2. Conservation of Mass for Smoke in a Control Volume (region enclosed by dashed lines).

PILOTED IGNITION

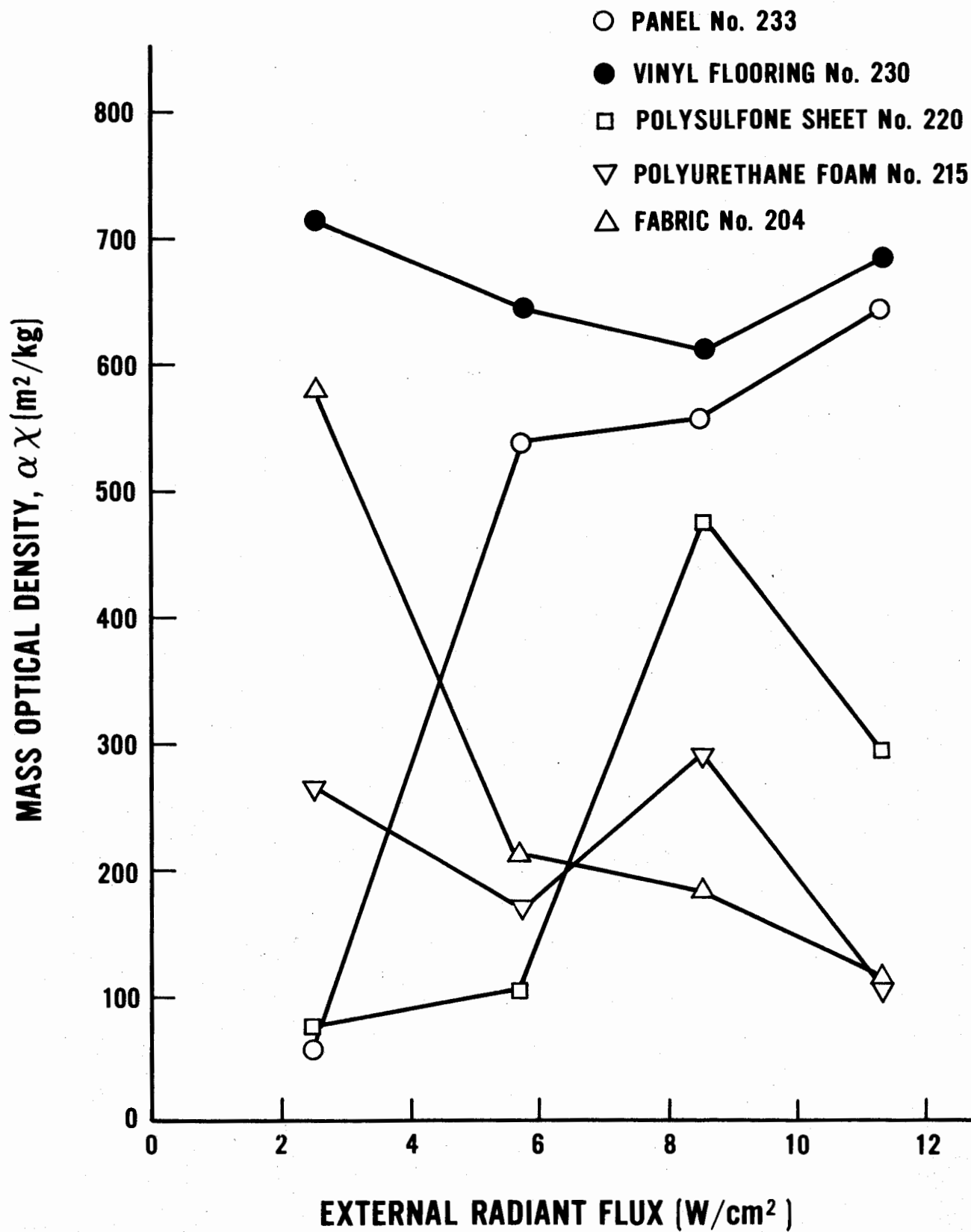


Figure 3. Mass Optical Density as a Function of Heat Flux Derived from Brown [23].

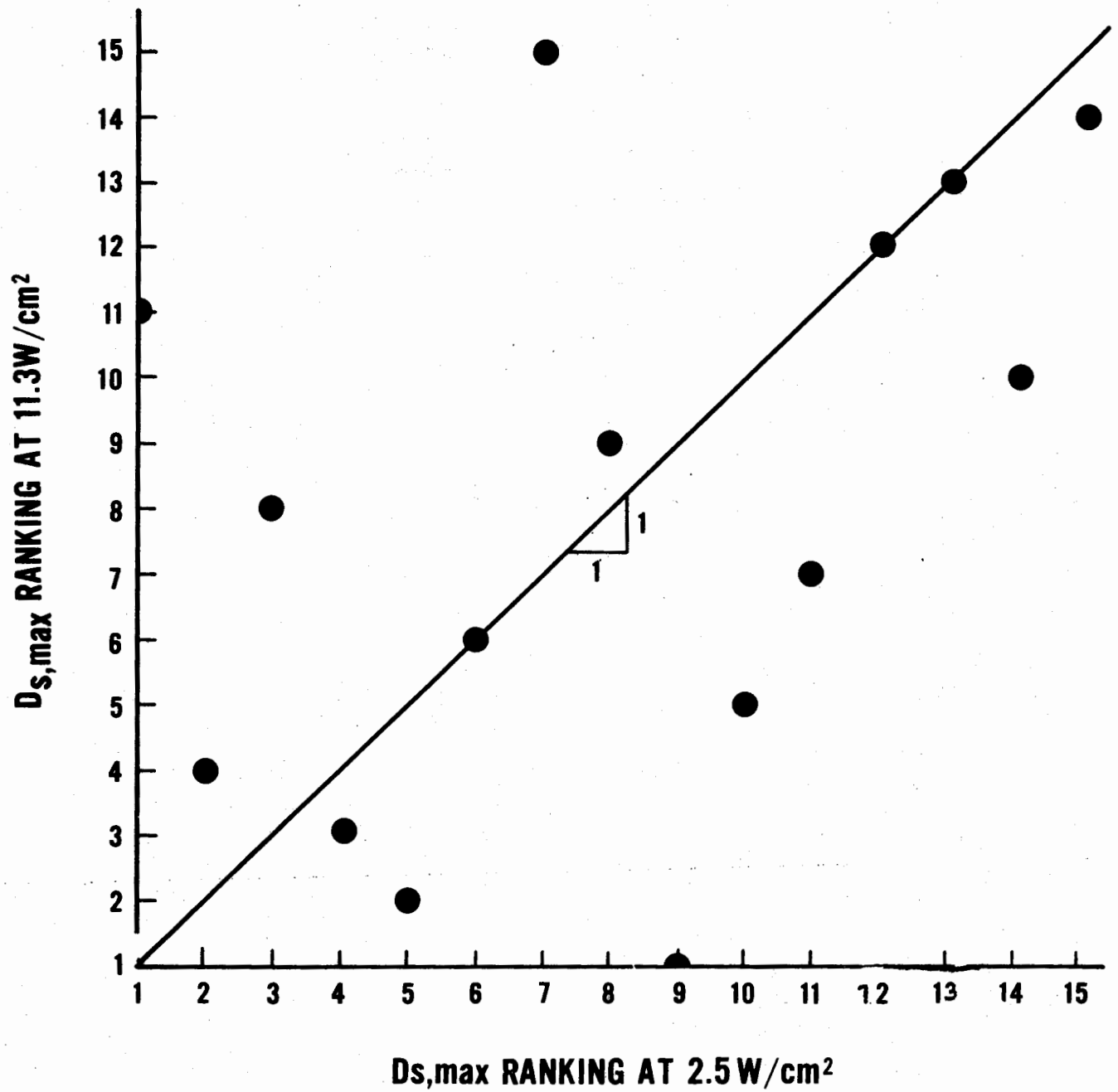


Figure 4. $D_{s,max}$ Rankings at two Flux Levels from Brown [23] for Piloted Ignition.

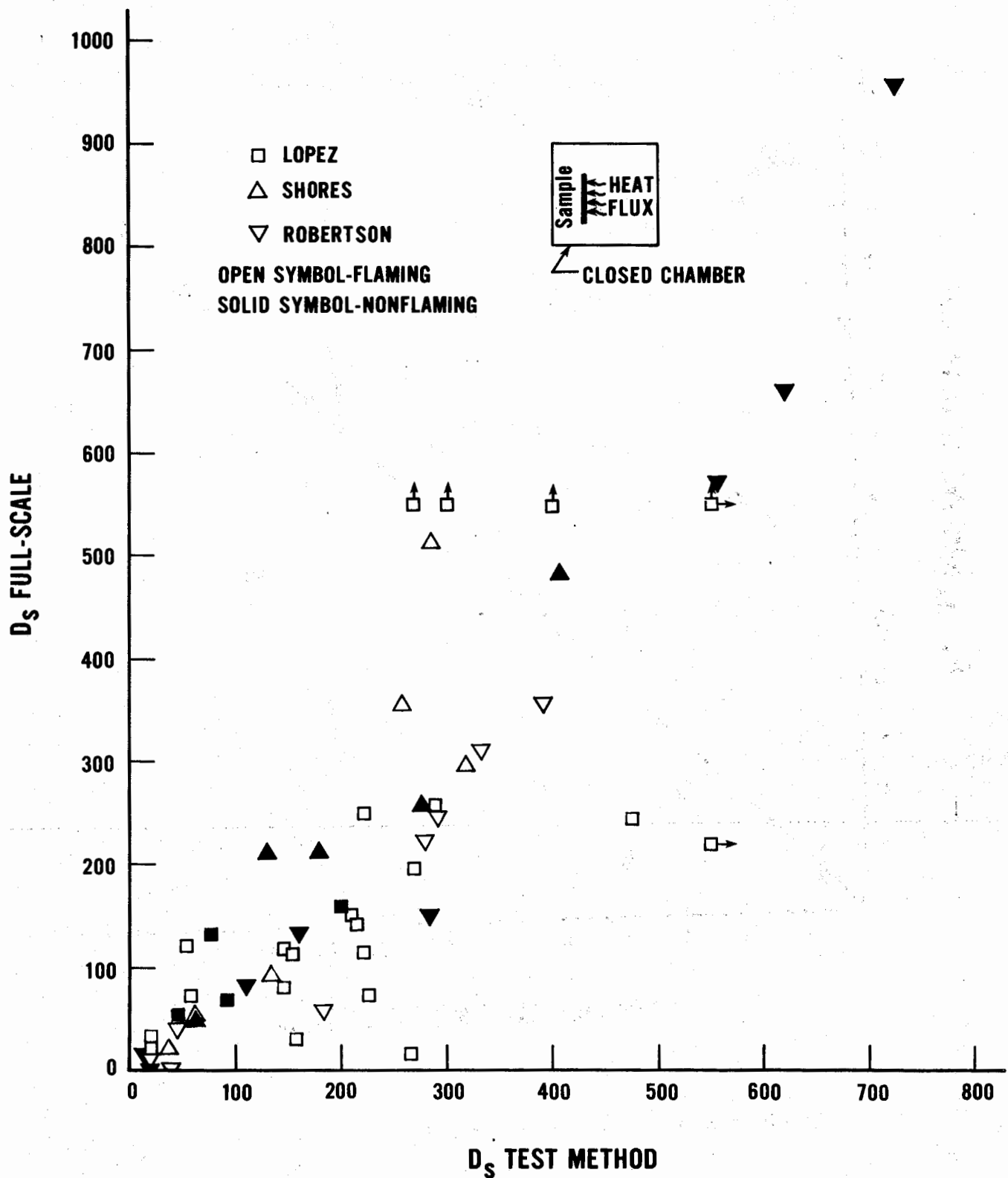


Figure 5 - $D_{s, \max}$ Compared for the Smoke Density Chamber and Large Closed Rooms from Lopez [1], Shores [32] and Robertson [33].

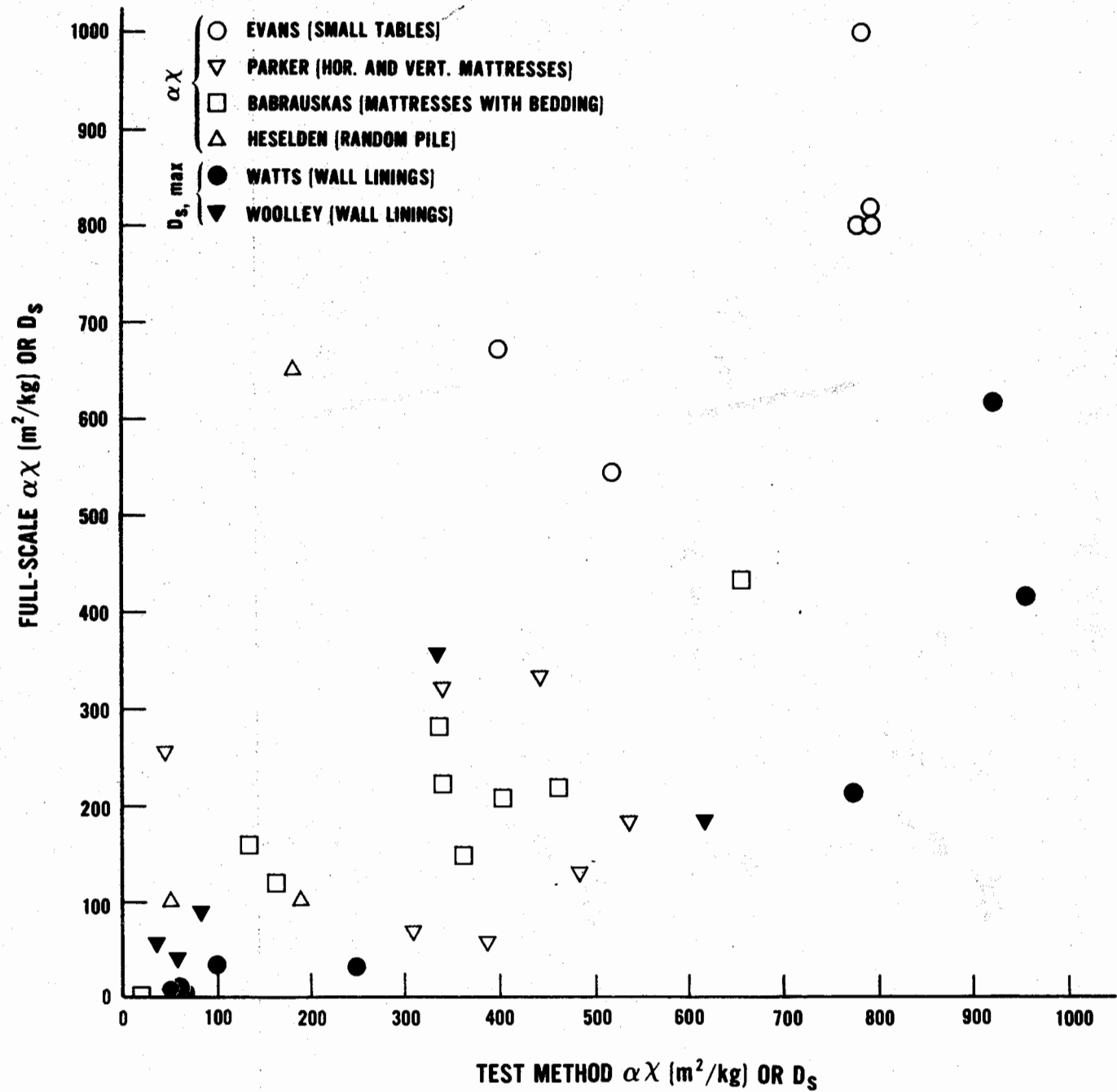


Figure 6 - Comparison Between Full-Scale and Test Method Results in Terms of Maximum Specific Optical Density ($D_{s,max}$) and Mass Optical Density ($\alpha\chi$).

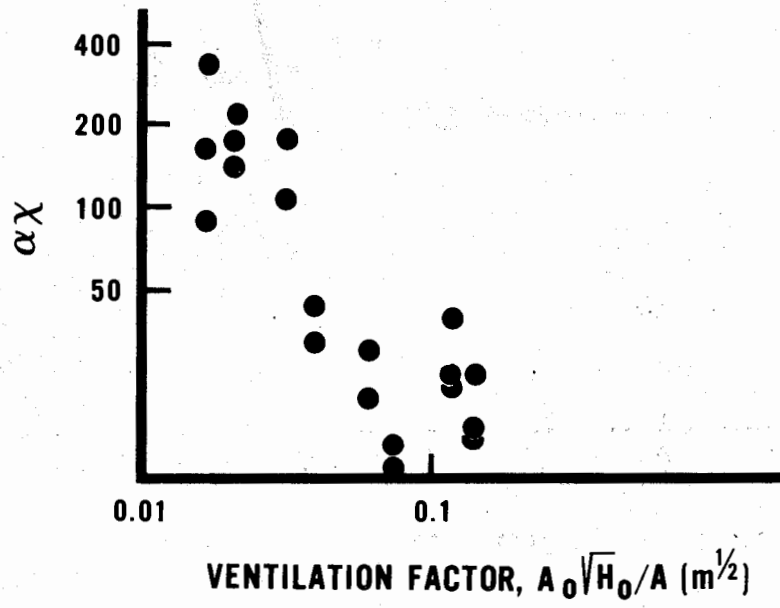
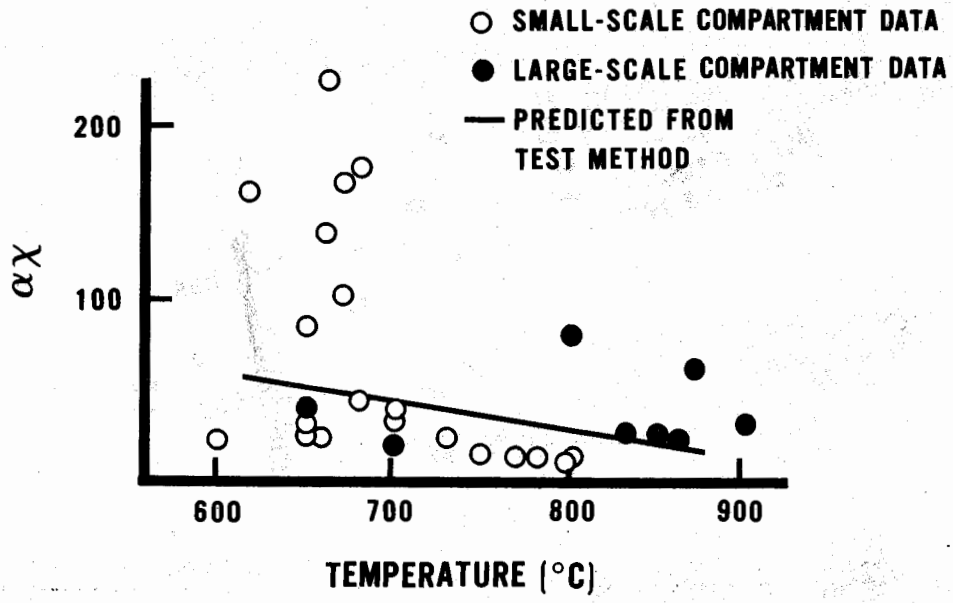


Figure 7 - Smoke Production for Plywood as a Function of Temperature (a) and Ventilation Factor (b) from Saito [24].

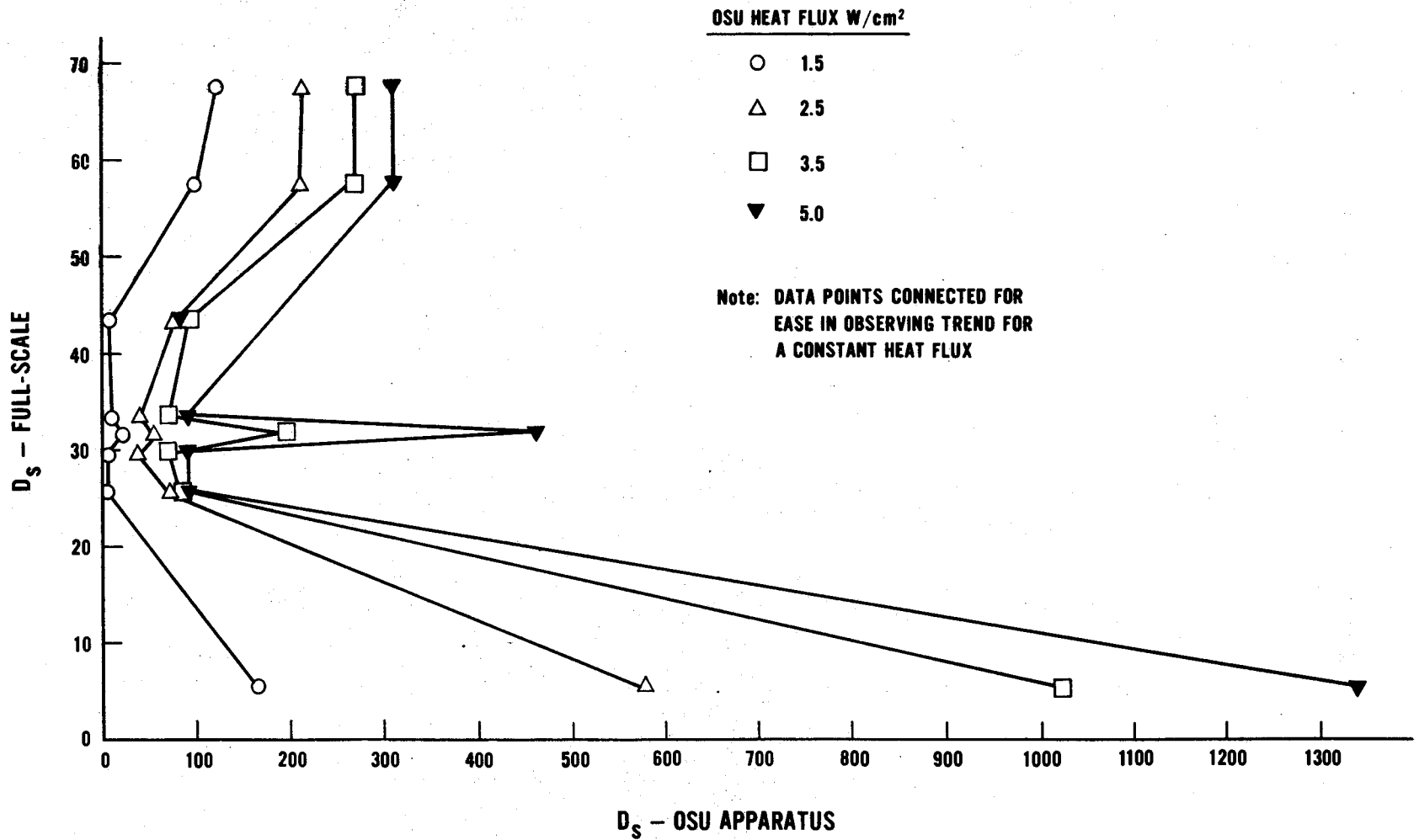


Figure 8. Full-Scale Smoke Compared to D_s from the OSU Combustibility Apparatus at Several Heat Flux Levels [21].

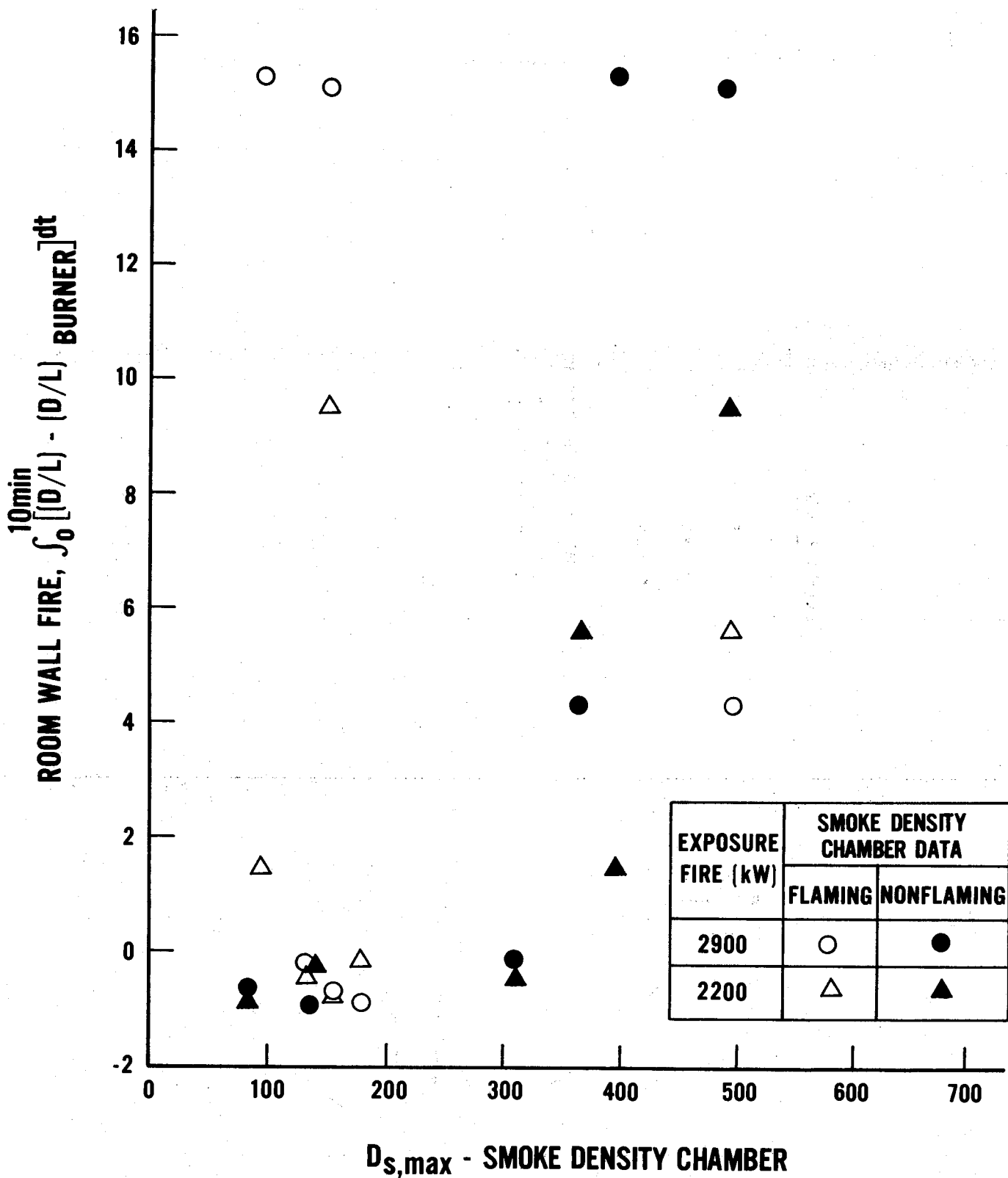


Figure 9 - Results from Room Lining Fires Compared to the Smoke Density Chamber from Christian and Waterman [42].

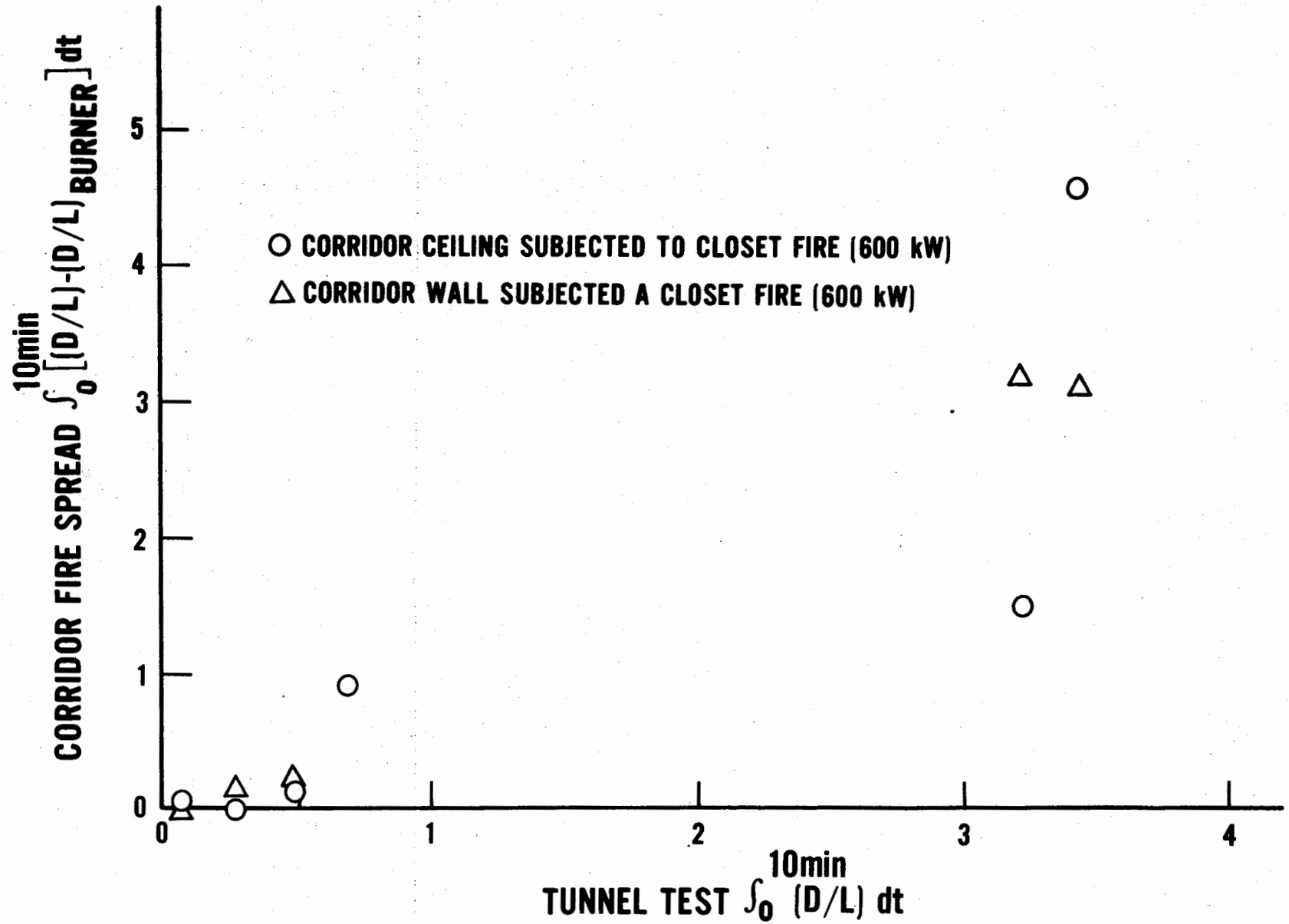


Figure 10. Smoke in Corridor Fire Spread Compared to Results Derived from the Steiner Tunnel Test from Christian and Waterman [42].

TUNNEL TEST CLASSIFICATION Δ

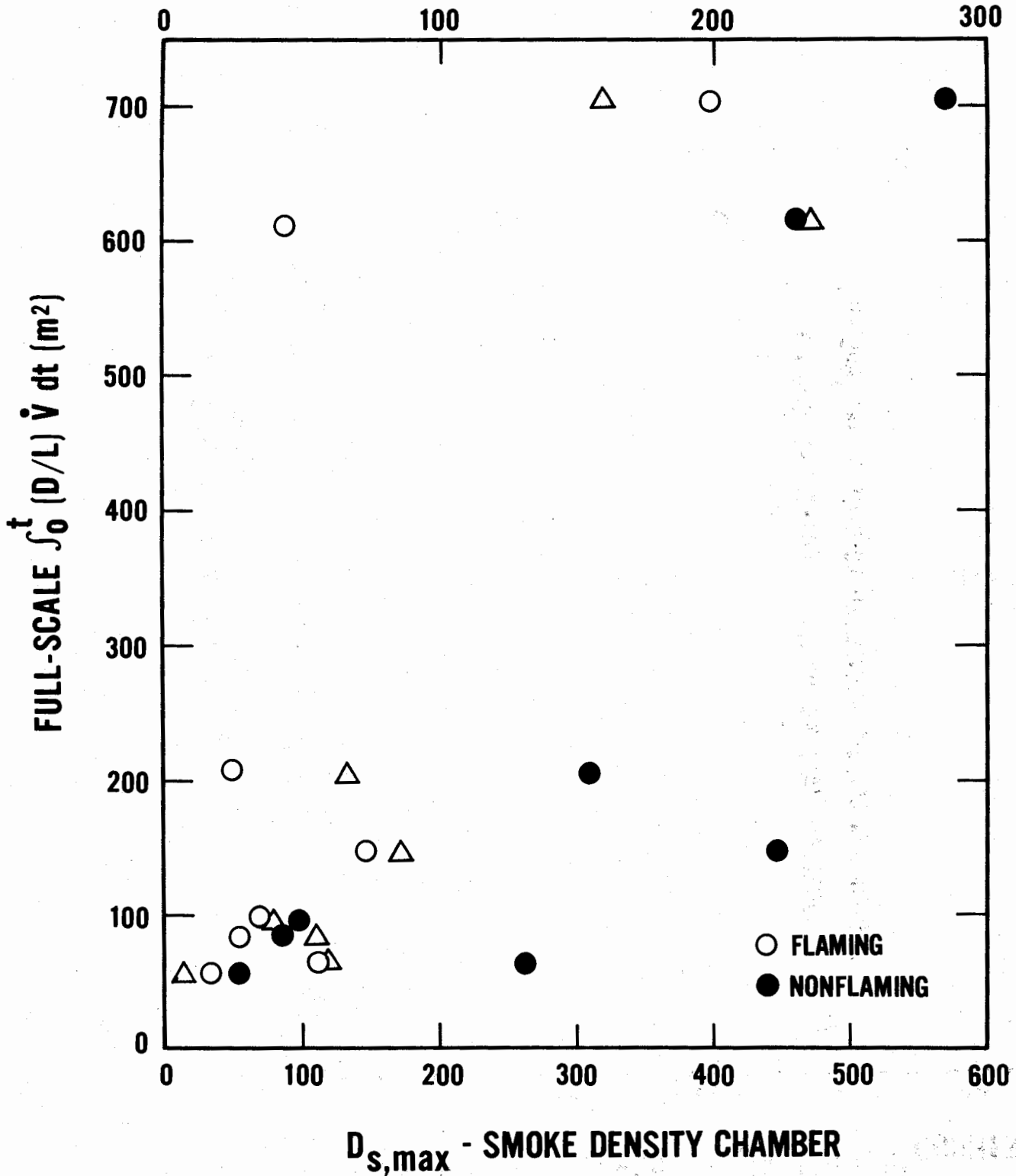


Figure 11 Lining Fires in Rooms and Smoke Data from the Smoke Density Chamber and the ASTM E-84 Tunnel Classification for Smoke from Fang [43].

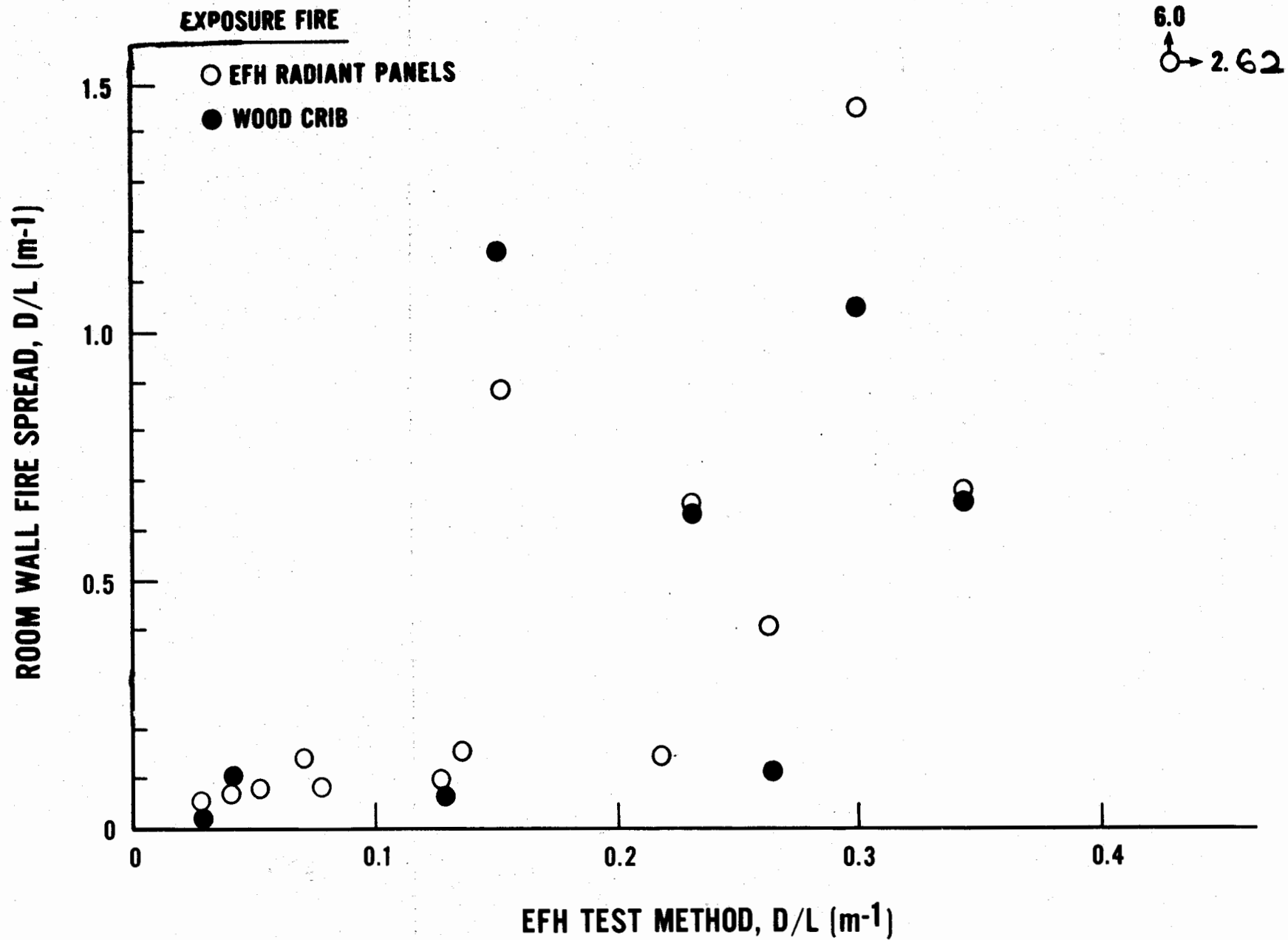


Figure 12. Smoke from Lining Fires in a Room Compared to the Early Fire Hazard (Australia) Test Method [44].

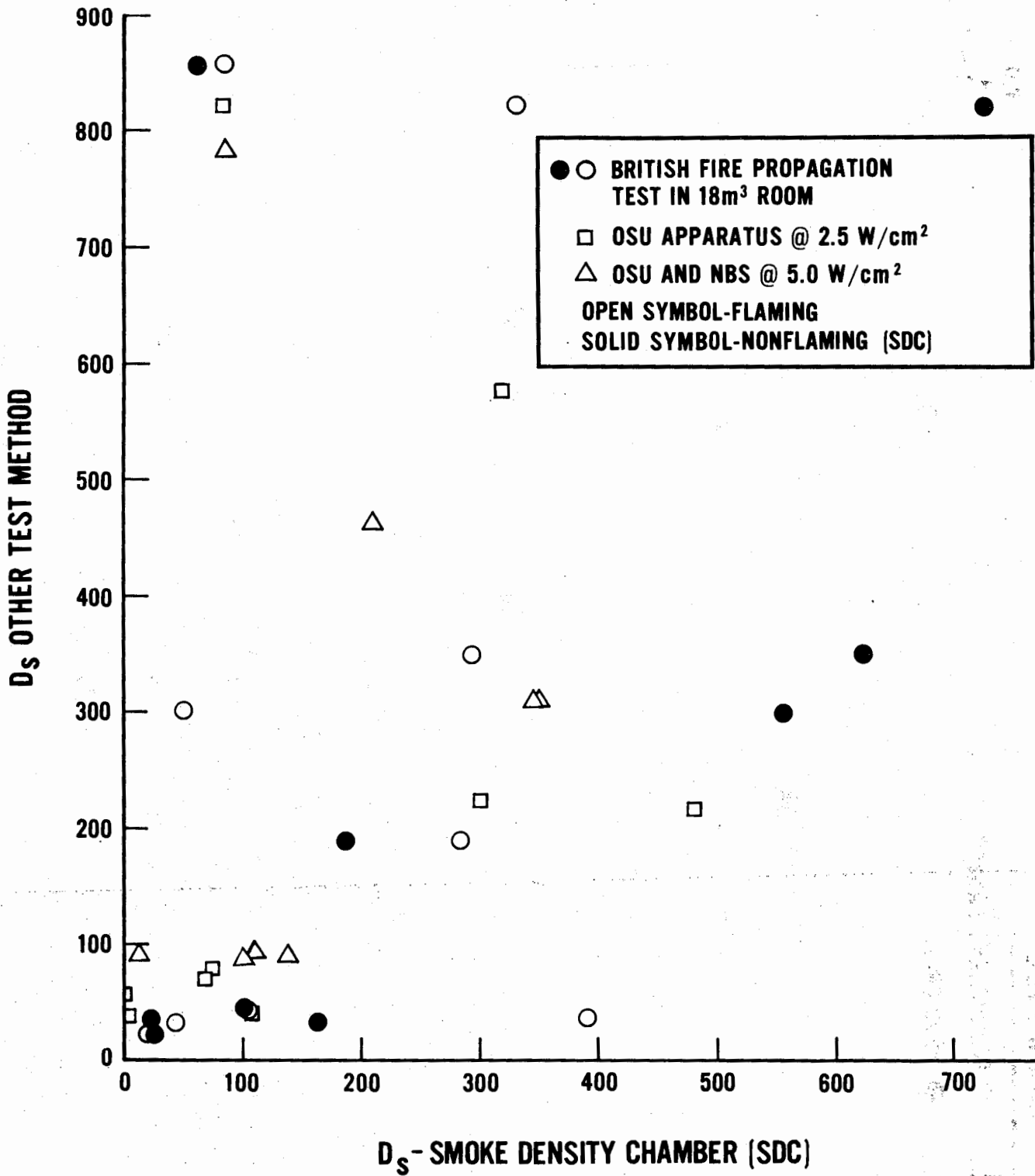


Figure 13 - Comparison of Smoke Density Chamber, OSU Combustibility Apparatus and British Smoke Test Data [21, 33].

APPENDIX

BRIEF DESCRIPTION OF LABORATORY TEST METHODS FOR SMOKE DATA

SMOKE DENSITY CHAMBER. [47]

A vertical sample is decomposed under 2.5 W/cm^2 irradiance with or without an igniting pilot flame in a closed chamber. The optical density is measured over a vertical path length in the chamber.

OHIO STATE COMBUSTIBILITY APPARATUS. [48]

A steady-flow system is used in which the optical density is measured in the exhaust system. Typically a vertical sample is decomposed under a prescribed irradiance level.

STEINER TUNNEL TEST. [49]

A relatively large sample is mounted on the ceiling of a rectangular horizontal duct in which a diffusion flame initiates flame spread and burning of the material. The light transmission is recorded for the exhaust gases, and the integral of $[1-I(L)/I(0)]$ over time is normalized with that found for red oak as a classification index.

ARAPAHOE SMOKE. [50]

A small sample inclined at 10° is subjected to a propane burner flame for 30 s and smoke is collected in the effluent stream by a filter for a total of 60 s.

BRITISH FIRE PROPAGATION/SMOKE TEST. [51]

A vertical sample forming a wall of a small vented box is subjected to an impinging flame for 20 minutes and additional radiant heat after 2.75 minutes. The smoke from the box is circulated in a room ($\sim 18 \text{ m}^3$) and the optical density is measured.

AUSTRALIAN EARLY FIRE HAZARD TEST. [52]

The sample is exposed to a 800° radiant panel at decreasing distances until ignition occurs after which the maximum optical density is measured over a one minute period by light path through the stack over the apparatus.

SUMMARY OF $D_{s,max}$ AND $\alpha\chi$ DATA FROM LARGE SCALE AND TEST METHOD-BASED EXPERIMENTS

Tables A-1 through A-6 list the computed values for D_s or $\alpha\chi$. The corresponding test apparatuses and full-scale fire test configurations are displayed in Figure A1. The formulae used in these computations are listed and are consistent with Eqns. (15) and (17) and the configurations in Figure A-1.

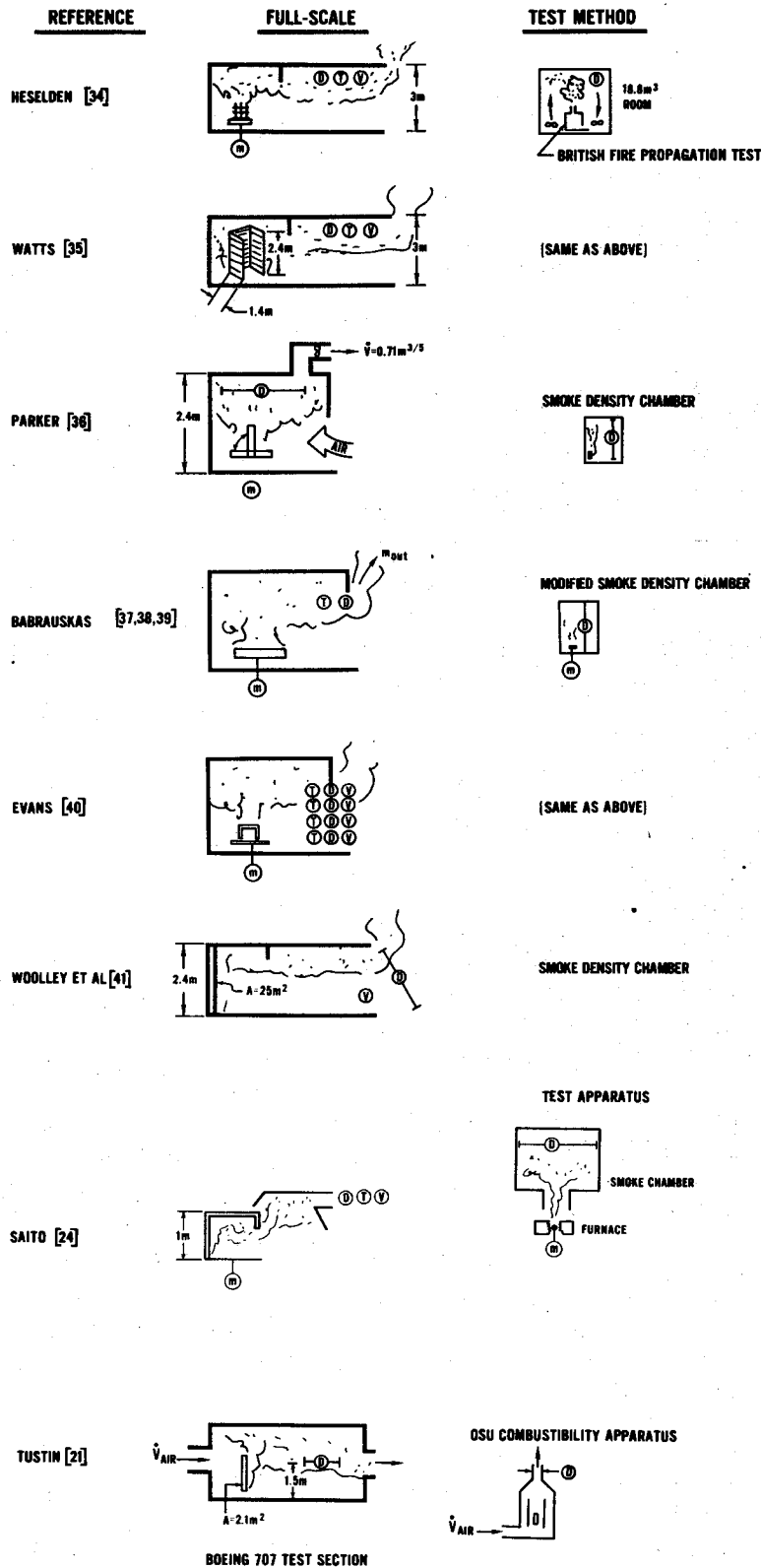


Figure A-1 - Full-Scale Test Configurations and Test Method Apparatus Used in Correlation. Symbols Denote Measurement Locations: D-Light Transmission, T-Temperature, V-Velocity, m-Mass Loss.

TABLE A-1. DATA FROM HESELDEN [34]

<u>Test Number</u>	<u>Material</u>	<u>Full-Scale</u>	<u>Test Method</u>
		$\alpha\chi = \frac{\int_0^t (D/L)\dot{V}dt}{\Delta m_f} \quad \frac{m^2}{kg}$	$\alpha\chi = \frac{(D_{max}/L)V}{m_o} \quad \frac{m^2}{kg}$
1	Wood	100 ¹	50
2	Polyurethane Foam	100 ²	190
3	Polystyrene	600-800 ³	180

¹ wood crib

² cushions

³ pieces in a pile

Table A-2. DATA FROM WATTS [35]

<u>Test Number</u>	<u>Material</u>	<u>Full-Scale</u>	<u>Test Method</u>
		$D_s = \frac{\int_0^t (D/L) \dot{V} dt}{A_{\text{(burned)}}$	$D_s = \frac{(D_{\text{max}}/L)V}{A_{\text{(burned)}}$
1	Expanded Polystyrene	3.8	43
2	Plasterborad, painted	1.0	63
3	Decorative laminate	4.8	68
4	Wood fibre board, painted	34	101 (1975 data)
			270 (1972 data)
5	Glass reinforced polyester		
	(a) polyester based intumescent coating	220	775
6	(b) water based intumescent coating	415	960
7	(c) no coating	620	920

TABLE A-3. DATA FROM PARKER [36]

<u>Test Number</u>	<u>Material</u>	<u>Full-Scale</u>	<u>Test Method</u>
		$\alpha_X = \frac{(D_{\max}/L)\dot{V}\Delta t}{\Delta m} \frac{m^2}{kg}$	$\alpha_X = \frac{D_{s,\max} A}{m_o} \frac{m^2}{kg}$
S2*	Polyurethane no. 2	257	47
U3	Polyurethane no. 1	129	490
T3	Neoprene	319	337
S3	Polyurethane no. 2	63	311
U4	Polyurethane no. 1	337	444
T4	Neoprene	186	535
S4	Polyurethane no. 2	60	394

* 2, 3, 4 denote different tickings
 2 - horizontal 3,4 - vertical

TABLE A-4. DATA FROM BABRAUSKAS [37-39]

<u>Test Number</u>	<u>Material</u>	<u>Full-Scale</u>	<u>Test Method</u>
		$\alpha\chi = \frac{\dot{m}_{out}}{(\rho_{\infty} T_{\infty} / T_g)} \frac{(D/L)^*}{\dot{m}}$ m^2/kg	$\alpha\chi = \frac{V}{L} \frac{dD}{dt} / \dot{m}$ m^2/kg
2-12	Fiberglass with Bedding	82.	-
2-3	M01 - Polyurethane	221.	328.
2-2	M02 - Polyurethane	145.	362.
2-1	M03 - Cotton	115.	166.
2-14	M04 - Latex	436.	653.
2-13	M05 - Polyurethane	87.	76.
2-11	M06 - Cotton, nylon, polyester	157.	132.
2-10	M07 - Cotton	0.	17.
2-8	M08 - Neoprene	203.	401.
2-6	M09 - Polyurethane	284.	338.
2-5	M10 - Neoprene	215.	467.

* evaluated at time when \dot{m} is maximum, also $\alpha\chi$ from control test (bedding) is subtracted for each material

Table A-5. DATA FROM WOOLLEY, RAFTERY, AMES, MURRELL [41]

<u>Test Number</u>	<u>Material</u>	<u>Full-Scale</u>	<u>Test Method</u>	
			$D_{s,max}$	
		$D_s = \frac{\int_0^{t_f} (\frac{D}{L}) \dot{V} dt^*}{A}$		
			Angled Jets	Horizontal Jets
1	Chipboard	365	390	334
2	Fire Insulation Board	33	77	58
3	Polystyrene	63	222	32
4	Plasterboard	~0	88	52
5	Glass reinforced polyester	183	651	616
6	Hardboard	86	79	77

*wood crib smoke subtracted

TABLE A-6. DATA FROM EVANS [4]

Full-Scale

Test Method

<u>Test Number</u>	<u>Material</u>	<u>Full-Scale</u>	<u>Test Method</u>
		$\alpha_X = \frac{\int_0^{t_f} \int_0^{S(\text{out})} (D/L)v \, dSdt}{\Delta m_f} \frac{\text{m}^2}{\text{kg}}$	$\alpha_X = \frac{(D/L)V}{\Delta m_f} \frac{\text{m}^2}{\text{kg}}$
7	Polystyrene	1000.	785.
8	Polystyrene	800.	785.
11	Polypropylene	670.*	400.
16	Polystyrene foam	820.	790.
17	Polystyrene foam	800.	790.
18	ABS	540.	520.

* questionable, may be too high

TABLE A-7. DATA FROM TUSTIN [12]

Test Number	Material	Full-Scale	NBS Smoke Chamber		OSU Combustibility Apparatus			
			2.5 W/cm ²	5.0 W/cm ²	1.5 W/cm ²	2.5 W/cm ²	3.5 W/cm ²	5.0 W/cm ²
Post Crash Simulation, t=90s*								
		$D_s = \frac{\alpha \int_0^t \dot{m}_s dt}{A}$		$D_s(t) = \frac{DV}{LA}$		$D_s(t) = \frac{\int_0^t (\frac{D}{L}) \dot{V} dt}{A}$		
N02/N03		57.7	300.	350.	100.	212.	270.	310.
402/403		43.8	75.	105.	7.	79.	88.	82.
412/413		31.9	0.	210.	20.	56.	197.	462.
416/417		29.7	3.	15.	7.	38.	70.	90.
Inflight Fire Simulation, t=300s†								
N02/N03		67.3	480.	350.	122.	215.	270.	310.
402/403		25.7	70.	110.	7.	70.	85.	90.
412/413		5.6	315.	640.	168.	576.	1025.	1450.
416/417		33.2	110.	140.	10.	40.	70.	90.

*Post Crash Simulation: 17 kg/min. air flow, flux to 8.9 W/cm²

†Inflight Simulation: 50.8 kg/min. air flow, flux to 4.2 W/cm²

U.S. DEPT. OF COMM. BIBLIOGRAPHIC DATA SHEET (See instructions)		1. PUBLICATION OR REPORT NO. NBSIR 82-2508	2. Performing Organ. Report No. DOT/FAA/CT-82/100	3. Publication Date July 82
4. TITLE AND SUBTITLE An Assessment of Correlations Between Laboratory and Full-Scale Experiments for the FAA Aircraft Fire Safety Program, Part 1: Smoke				
5. AUTHOR(S) James G. Quintiere				
6. PERFORMING ORGANIZATION (If joint or other than NBS, see instructions) NATIONAL BUREAU OF STANDARDS DEPARTMENT OF COMMERCE WASHINGTON, D.C. 20234			7. Contract/Grant No.	8. Type of Report & Period Covered
9. SPONSORING ORGANIZATION NAME AND COMPLETE ADDRESS (Street, City, State, ZIP) Federal Aviation Administration Technical Center Atlantic City, N.J. 08405				
10. SUPPLEMENTARY NOTES <input type="checkbox"/> Document describes a computer program; SF-185, FIPS Software Summary, is attached.				
11. ABSTRACT (A 200-word or less factual summary of most significant information. If document includes a significant bibliography or literature survey, mention it here) An extensive review is presented demonstrating the nature of comparison between full-scale fire smoke data and test method results for materials. These correlations are presented in terms of consistent parameters established through a development of the governing equations for smoke concentration and light attenuation. Visibility data pertaining to light transmission through smoke is presented but no general results exist on the sensory irritant effect of smoke on vision. Analysis shows the complex dependence of smoke production on many parameters acting in fire growth and shows the futility and nature of simple correlation attempts. Recommendations are made for further research to establish a sounder basis for correlations, and a practice strategy is suggested for proceeding in the present.				
12. KEY WORDS (Six to twelve entries; alphabetical order; capitalize only proper names; and separate key words by semicolons) Correlation; full-scale; fire tests; smoke; smoke density chamber; optical density; test methods; visibility.				
13. AVAILABILITY <input checked="" type="checkbox"/> Unlimited <input type="checkbox"/> For Official Distribution. Do Not Release to NTIS <input type="checkbox"/> Order From Superintendent of Documents, U.S. Government Printing Office, Washington, D.C. 20402. <input checked="" type="checkbox"/> Order From National Technical Information Service (NTIS), Springfield, VA. 22161			14. NO. OF PRINTED PAGES 53	
			15. Price \$9.00	